



ELSEVIER

Advanced Drug Delivery Reviews 37 (1999) 189–211

advanced  
**drug delivery**  
reviews

# Utilization of metabolic, transport and receptor-mediated processes to deliver agents for cancer diagnosis

Cathy S. Cutler, Jason S. Lewis, Carolyn J. Anderson\*

*Mallinckrodt Institute of Radiology, Washington University School of Medicine, 510 S. Kingshighway, Campus Box 8225, St. Louis, MO 63110, USA*

## Abstract

The use of radiopharmaceuticals for the non-invasive diagnosis of cancer has been established in diagnostic radiology over the last few decades. In particular, with the use of sophisticated imaging modalities such as PET and SPECT and a myriad of radioisotopes, advances have been made in the detection and treatment of cancer. This article focuses on three available methods of tumor targeting with radiopharmaceuticals: the utilization of metabolic, transport and receptor-mediated processes to deliver agents for cancer diagnosis. With selected reference to both clinically approved drugs and drugs currently under development, methods of uptake are presented either in terms of flow, metabolic or receptor mediated uptakes. A section of this article is devoted to the monitoring of cancer therapy regimes using radiopharmaceuticals. This review also discusses some mechanistic approaches available in radiopharmaceutical chemistry to be able to effectively diagnose and treat sufferers of cancer in the future. © 1999 Elsevier Science B.V. All rights reserved.

*Keywords:* PET; SPECT; Radiopharmaceuticals; Cancer; Tumor; Diagnosis; Imaging

## Contents

1. Introduction .....	190
2. Flow and membrane transport based imaging agents .....	191
2.1. Oxygen-15-labeled radiopharmaceuticals .....	192
2.2. Cu-thiosemicarbazones .....	192
2.3. Thallium-201 .....	192
3. Metabolism-based radiopharmaceuticals .....	193
3.1. Bone imaging agents .....	193
3.2. 2-[ <sup>18</sup> F]fluoro-2-deoxyglucose (FDG) .....	194
3.3. Amino acids .....	195
4. Receptor and transport-mediated radiopharmaceuticals .....	196
4.1. <sup>67</sup> Ga- and <sup>68</sup> Ga-citrate .....	196
4.2. MIBG .....	197
4.3. Somatostatin analogs .....	198
4.4. Steroid receptor ligands .....	200
5. Monitoring cancer therapy with radiopharmaceuticals .....	201

\*Corresponding author. Tel.: + 1-314-362-8427; fax: + 1-314-362-9940.

*E-mail address:* andersoncj@mirlink.wustl.edu (C.J. Anderson)

5.1. Monitoring hormonal therapy with FES .....	201
5.2. Multi-drug resistance .....	201
5.3. Imaging of tumor hypoxia .....	202
6. Summary and conclusion .....	204
7. Glossary .....	204
Acknowledgements .....	205
References .....	205

## 1. Introduction

Radiopharmaceuticals have been used extensively in the field of nuclear medicine as non-invasive diagnostic imaging agents to provide both functional and structural information about organs and diseased tissues [1–6]. Nuclear medicine imaging is considerably more sensitive than most other imaging modalities (X-ray, CT, MRI) for identifying the presence and extent of malignancy, since biochemical changes monitored by positron emission tomography (PET) and single photon emission computed tomography (SPECT) generally precede anatomical changes.

Radiopharmaceuticals consist of either a gamma- or a positron-emitting radionuclide bound to ligands which cause selective accumulation in cancerous or diseased tissue following intravenous injection [6]. In cancer diagnoses the effectiveness of these radiopharmaceuticals is ultimately determined by their selectivity for cancerous versus normal tissue. Tumors frequently exhibit differences in blood flow, glycolysis or nucleic acid synthesis, increase in concentration of specific receptors or an overall increase in metabolism compared to the tissue of origin. Radiopharmaceuticals are designed to utilize these differences to concentrate selectively and specifically in malignant tissue.

The choice of radionuclide used to label the radiopharmaceutical is important when considering the mode of diagnostic imaging of cancer. In Tables 1 and 2 the wide variety of gamma and positron emitting radionuclides, their decay characteristics and methods of production are shown. In designing radiopharmaceuticals, important factors to consider include the half-life of the radionuclide, the mode of decay, and the cost and availability of the isotope. For diagnostic imaging, the half-life of the radionuclide must be long enough to allow the synthesis of the radiopharmaceutical, but short enough to limit

the dose to the patient. Radionuclides used in PET and gamma scintigraphy range in half-life from about 2 min ( $^{15}\text{O}$ ) to several days ( $^{67}\text{Ga}$ ). The optimal half-life depends on the time required for the radiopharmaceutical to localize in the target tissue. For example, perfusion-based radiopharmaceuticals can use shorter half-lives, since they reach the tumor quickly, whereas radiolabeled large proteins or monoclonal antibodies (mAbs) often take longer for optimal target to background ratios.

The most popular radionuclides used in diagnostic imaging decay primarily by gamma emission, since gamma scintigraphy is the most commonly used modality. Radionuclides used in PET decay by positron emission. The use of radiopharmaceuticals for therapeutic applications (alpha ( $\alpha$ ) or beta ( $\beta^-$ ) emitters) is increasing, and many of these radionuclides also emit gammas or positrons for application in both therapy and imaging. Most gamma cameras are designed for specific energy windows, generally around 100–200 keV. Radionuclides with gamma energies outside this range may produce low-quality images with SPECT but are not used routinely.

Another important factor in choosing radionuclides for diagnostic imaging is their cost and availability. Radionuclide generators are considered ideal, since many of them are relatively inexpensive and have long shelf-lives. They consist of a longer-lived parent isotope decaying to a shorter-lived daughter radionuclide which is separated from the parent by ion exchange chromatography or solvent extraction. Even small hospitals can usually afford these generators. A few radiometals used for radiopharmaceuticals are produced by a nuclear reactor. These isotopes are generally affordable, since nuclear reactors can produce many isotopes at one time.

Accelerator or cyclotron radioisotopes are the more expensive mode of production, since only one isotope is produced at a time.

Table 1  
Gamma-emitting radionuclides

Isotope	$T_{1/2}$ (h)	Production methods	Decay mode	$E_{\gamma}$ (keV)	Reference
$^{67}\text{Ga}$	78.26	Cyclotron	EC (100%)	91, 93, 185, 296, 388	[191]
$^{123}\text{I}$	13.0	Cyclotron	EC	28, 159	[191]
$^{131}\text{I}$	193.4	Reactor	$\beta^-$	364	[191]
$^{99\text{m}}\text{Tc}$	6.0	$^{99}\text{Mo}/^{99\text{m}}\text{Tc}$ Generator	IT (100%)	141	[191]
$^{111}\text{In}$	67.9	Cyclotron, $^{111}\text{Cd}(\text{p},\text{n})^{111}\text{In}$	EC (100%)	245, 172	[191]

Table 2  
Positron-emitting radionuclides

Isotope	$T_{1/2}$ (h)	Methods of production	Decay mode	$E_{\beta^+}$ (keV)	Reference
$^{60}\text{Cu}$	0.4	Cyclotron, $^{60}\text{Ni}(\text{p},\text{n})^{60}\text{Cu}$	$\beta^+$ (93%) EC (7%)	3920, 3000 2000	[22,23,191]
$^{61}\text{Cu}$	3.3	Cyclotron, $^{61}\text{Ni}(\text{p},\text{n})^{61}\text{Cu}$	$\beta^+$ (62%) EC (38%)	1220, 1150 940, 560	[22,23,191]
$^{62}\text{Cu}$	0.16	$^{62}\text{Zn}/^{62}\text{Cu}$ Generator	$\beta^+$ (98%) EC (2%)	2910	[23,191]
$^{64}\text{Cu}$	12.8	Cyclotron, $^{64}\text{Ni}(\text{p},\text{n})^{64}\text{Cu}$	$\beta^+$ (19%) EC (41%) $\beta^-$ (40%)	656	[21,23,191]
$^{68}\text{Ga}$	1.1	$^{68}\text{Ge}/^{68}\text{Ga}$ Generator	$\beta^+$ (90%) EC (10%)	1880, 770	[191,192]
$^{18}\text{F}$	1.83	Cyclotron $^{18}\text{O}(\text{p},\text{n})^{18}\text{F}$	$\beta^+$ (97%) EC (3%)	635	[191]
$^{124}\text{I}$	100.3	Cyclotron $^{124}\text{Te}(\text{p},\text{n})^{124}\text{I}$	$\beta^+$ (25%) EC (75%)	2134, 1533	[191]
$^{15}\text{O}$	0.03	Cyclotron $^{14}\text{N}(\text{d},\text{n})^{15}\text{O}$	$\beta^+$ (99%)	1723	[191]
$^{86}\text{Y}$	14.7	Cyclotron, $^{86}\text{Sr}(\text{p},\text{n})^{86}\text{Y}$	$\beta^+$ (33%) EC (66%)	2335, 2019 1603, 1248 1043	[191]

Diagnostic imaging in oncology fulfils several purposes: to locate the tumor and any metastases; to plan treatment and therapy regimes; to monitor response to therapy; and to identify residual or recurrent tumor. Diagnosis and staging determine treatment options and prognosis of the disease. This review will primarily cover three types of tumor imaging agents: flow-, metabolism-, and receptor-based agents. Monoclonal antibody-based agents are discussed in other chapters in this book. This review provides an overview on some of the more established agents, and discusses some of the new developments. This is by no means exhaustive, but rather attempts to emphasize the importance of imaging agents in cancer diagnosis, treatment and

staging, demonstrate the progress made over the last 10–15 years, and predict future research directions.

## 2. Flow and membrane transport based imaging agents

The simplest mode of delivery of a radiopharmaceutical to tumors is through first-pass extraction from the blood stream. Radiopharmaceuticals have been developed based simply on being carried into the tumor by blood flow;  $^{15}\text{O}$ -labeled water is an example. Other agents are taken up by tumor cells due to a combination of blood flow and other factors, such as membrane transport. For example, cations

such as  $^{201}\text{Tl}^+$  are actively transported, while some lipophilic radiopharmaceuticals accumulate in tumors by passive diffusion. The advantages of tumor imaging using small molecules that are taken up by more simple mechanisms such as blood flow is the ease of preparing the agent and the short time-frame with which images can be obtained. A disadvantage of these agents is they are by nature non-specific and usually show high-accumulation in other non-target organs as well. In this section we will cover a few examples of this class of compounds.

### 2.1. Oxygen-15-labeled radiopharmaceuticals

Oxygen-15-labeled  $^{15}\text{O}[\text{O}_2]$ ,  $^{15}\text{O}[\text{CO}_2]$  and  $^{15}\text{O}[\text{CO}]$  and PET have been used to determine regional blood flow and oxygen utilization in tumors, and also to monitor the response to therapeutic intervention; however, the blood flow in the tumors was highly variable due to inherent heterogeneity in brain tumor tissue [7]. In another study, tissue heterogeneity resulted in the underestimation of the mean values of oxygen extraction [8]. In gliomas, PET revealed a persistent depression of oxygen metabolism as indicated by the regional oxygen extraction fraction in the regions where the tumors were found [9].

Oxygen-15-labeled  $\text{H}_2^{15}\text{O}$  has been used to measure regional blood flow, because of a linear relationship between true flow and the tissue counts in a region of interest [10]. More recently,  $\text{H}_2^{15}\text{O}$  was utilized as a tumor blood flow tracer in combination with other oncological imaging agents. The uptake of  $\text{H}_2^{15}\text{O}$  and  $^{18}\text{F}$ -labeled fluorouracil ( $^{18}\text{F}$ -FU), a radio-labeled analog of a standard chemotherapeutic, have been compared as non-metabolizable and metabolizable tracers [11]. Comparison of these two tracers by intravenous versus intra-arterial administration showed that intra-arterial administration improved the access of fluorouracil in 87% of tumor metastases [12].  $\text{H}_2^{15}\text{O}$  has also been used in functional mapping of the location of gliomas prior to PET imaging with  $^{11}\text{C}$ -labeled methionine [13].

### 2.2. Cu-thiosemicarbazones

Bis(thiosemicarbazones) were discovered to possess anti-tumor properties in the 1960's [14]. It was

then found that the anti-tumor activity of the Cu(II) complexes of these ligands was significantly enhanced over the activity of the ligands alone [15]. These neutral, lipophilic complexes are rapidly taken up by cells, and the Cu(II) is reduced to Cu(I) by intracellular thiols (probably glutathione) [15,16]. The Cu(I) complexes are unstable and the copper dissociates and binds to intracellular proteins.

There are a number of copper radionuclides ( $^{60}\text{Cu}$ ,  $^{61}\text{Cu}$ ,  $^{62}\text{Cu}$  and  $^{64}\text{Cu}$ ) available for use in nuclear medicine imaging (Table 2). Copper-62 is available from two generator systems [17,18] and commercialization of these generators is currently underway [19,20]. The radionuclides  $^{60}\text{Cu}$ ,  $^{61}\text{Cu}$  and  $^{64}\text{Cu}$  can all be produced in large quantities with high yields on small biomedical cyclotrons [21,22]. For a more comprehensive review on copper radionuclides and copper bis(thiosemicarbazones), please see the review by Blower et al. [23]. The most widely used in research are the positron-emitting  $^{62}\text{Cu}$  ( $T_{1/2} = 9.8$  min) and  $^{64}\text{Cu}$  ( $T_{1/2} = 12.8$  h). Because the Cu(II)bis(thiosemicarbazones) demonstrated rapid diffusion into cells followed by trapping of the Cu(I/II) ion, these agents were labeled with copper radionuclides and evaluated as possible radiopharmaceuticals for myocardial and cerebral perfusion imaging [24]. Several structural analogs of the bis(thiosemicarbazones) were evaluated as blood flow tracers, and one analog, Cu(II)pyruvaldehyde bis( $N^4$ -methylthiosemicarbazone) (Cu-PTSM), was chosen for further evaluation [25] (Fig. 1). Cu-PTSM was found to have 'microsphere-like' kinetics since it is non-tissue selective and rapidly extracted from the blood [26]. This agent was evaluated in two tumor-bearing animal models and found to show proportional uptake to  $^{125}\text{I}$ -labeled antipyrine, which is a known blood flow agent [27]. The high lipophilicity which results in high liver uptake and slow hepatobiliary clearance makes intravenously administered Cu-PTSM a less than ideal flow tracer for routine tumor blood flow imaging; however this tracer has potential application as a radiotherapeutic when injected intratumorally.

### 2.3. Thallium-201

Thallium-201 ( $t_{1/2} = 73.1$  h) results from the decay of  $^{201}\text{Pb}$ . Suitable SPECT images can be

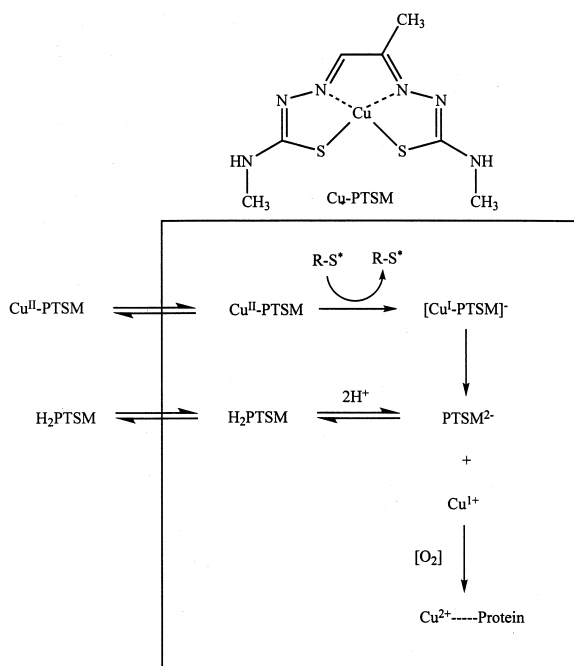


Fig. 1. Structure of Cu(II)pyruvaldehyde bis(*N*<sup>4</sup>-methylthiosemicarbazone) (Cu-PTSM), and the mechanism of trapping inside tumor cells.

obtained, despite the low energy X-rays (63–85 keV) emitted. Interest in  $\text{Tl}^+$  arose from its similarities to  $\text{K}^+$ , which include their similar hydrated ionic radius, common ionic charge and distribution in the body. Most importantly,  $\text{Tl}^+$  binds to the Na–K-ATPase pump and its intracellular uptake is blocked by known inhibitors of the Na–K-ATPase pump [28,29]. The cellular uptake of  $\text{Tl}^+$  is also related to both sodium and glucose transport across the cell membrane [30].  $^{201}\text{Tl}$  as a potassium analog was originally used as a myocardial imaging agent, and its uptake and redistribution in myocardium is used to measure myocardial perfusion and viability.

The exact mechanism of uptake of  $^{201}\text{Tl}$  in tumor cells is not clearly defined. Tumor uptake has been shown to be dependent on blood flow and the  $\text{Na}^+/\text{K}^+$  pump [30]. Other contributing factors include tumor viability, type of malignancy, ion co-transport system, calcium ion channel exchange, vascular immaturity with leakage and increased cell permeability and tumor necrosis [31–34].

$^{201}\text{Tl}$  chloride uptake in brain tumors, including

malignant gliomas, astrocytomas, and ependymomas, differentiates recurrent brain tumors from residual mass and correlates with 2- $^{18}\text{F}$ fluoro-2-deoxyglucose (FDG) PET studies [35–38]. The combination of  $^{67}\text{Ga}$  and  $^{201}\text{Tl}$  scans can differentiate between infection and malignancy. For example, a negative  $^{201}\text{Tl}$  scan with a positive  $^{67}\text{Ga}$  scan indicates inflammation or infection. In AIDS patients with lung lesions, thallium in combination with gallium has been used to distinguish infection from neoplasms [39]. Kaposi's syndrome and lymphoma incorporate  $^{201}\text{Tl}$  whereas infection does not [39].  $^{201}\text{Tl}$  SPECT imaging has also been shown to be useful in distinguishing malignant intracranial lymphoma from non-malignant lesions such as toxoplasmosis and multifocal leukoencephalopathy in AIDS patients [40]. A study comparing the abilities of  $^{99\text{m}}\text{Tc}$ -MDP,  $^{67}\text{Ga}$ -Citrate and  $^{201}\text{Tl}$  to predict tumor response to therapy in patients with bone and soft-tissue sarcoma showed  $^{201}\text{Tl}$  to be superior [41]. The superiority of  $^{201}\text{Tl}$  is attributed to its ability to directly assess tumor cell avidity.

### 3. Metabolism-based radiopharmaceuticals

Metabolic imaging depends on the accelerated metabolism in tumor versus normal tissue. Increased utilization of glucose, DNA or amino acids mark the transformed cell, with the rate of increase roughly corresponding to the rate of tumor growth. Radio-labeled glucose analogs, amino acids and nucleotides have been successfully used for metabolism-based tumor imaging. Bone imaging agents take advantage of the changes in bone metabolism that result from tumor growth in the bone. In this section, we discuss some radiotracers for metabolic imaging and their modes of delivery.

#### 3.1. Bone imaging agents

Of patients diagnosed with breast, prostate or lung cancer, 50% eventually develop skeletal metastases [42,43]. The most frequently requested diagnostic nuclear medicine procedure is the  $^{99\text{m}}\text{Tc}$ -methylene diphosphonate (MDP) bone scan. The bone-scan, unlike X-ray procedures which reflect mineral con-

tent, outlines physiological processes such as the functional reaction of bone to traumatic, inflammatory, or neoplastic injury [44] which leads to an increase in new bone formation and an increase in skeletal blood flow. Therefore, bone-seeking complexes concentrate in skeletal lesions, giving a higher lesion to normal bone ratio (L/NB) and enhanced visualization. The metabolism of the tumor cells themselves does not cause increased uptake, but instead is directly related to local changes in bone metabolism resulting from tumor invasion. The  $^{99m}\text{Tc}$ -MDP bone scan can detect lesions long before radiographs of the skeleton become abnormal.

The ability of diphosphonates to function as bone seekers presumably arises from their ability to function as bidentate bridges [45,46]. This bidentate character permits the ligands to bridge two metal centers; e.g.  $^{99m}\text{Tc}$  and the calcium of hydroxyapatite. Subsequent studies of the fundamental chemistry of Tc-diphosphonate formulations revealed a complicated, time-dependent mixture of unidentified components rather than a single chemical species [47–49]. The  $^{99m}\text{Tc}$  labeled diphosphonates show fast blood clearance, reduced soft tissue uptake and increased normal bone uptake. The first diphosphonate used clinically as a  $^{99m}\text{Tc}$  bone scanning agent was 1-hydroxyethylidene diphosphonate (HEDP) which was eventually replaced by MDP due to its faster blood clearance and higher skeletal affinity [44] (Fig. 2a).

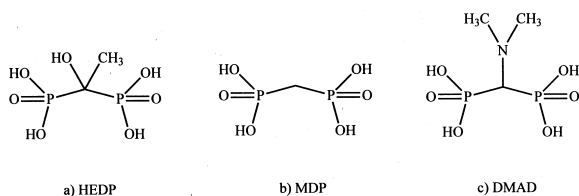


Fig. 2. Phosphonate ligands for labeling with  $^{99m}\text{Tc}$  which image bone metastases.

Several new diphosphonates have been developed as bone scanning agents. Only one of these agents is significantly better than  $^{99m}\text{Tc}$ -MDP (Fig. 2b).  $^{99m}\text{Tc}$ -dimethyleneaminomethylene diphosphonate (DMAD) (Fig. 2c) has a higher L/NB ratios in rats than MDP or hydroxymethylene diphosphonate (HMDP), [50,51] apparently due to the low normal bone uptake of  $^{99m}\text{Tc}$ -DMAD. Clinical studies comparing  $^{99m}\text{Tc}$ -MDP to  $^{99m}\text{Tc}$ -DMAD have concluded that all lesions detected by  $^{99m}\text{Tc}$ -MDP were also detected by  $^{99m}\text{Tc}$ -DMAD and that several lesions observed on the DMAD scan were not seen by MDP [52,53].

### 3.2. 2-[ $^{18}\text{F}$ ]fluoro-2-deoxyglucose (FDG)

FDG is utilized widely in many aspects of PET diagnostic medicine including cancer diagnosis and diseases of the brain and heart. The mechanism of FDG trapping follows the well documented glucose biochemical pathway. FDG is transported in the cell and is metabolized in the glycolytic system by phosphorylation by hexokinase to FDG-6-phosphate (Fig. 3). However, unlike glucose, FDG-6-phosphate is then trapped in the cell due to the very strict stereochemical and structural demands of the enzyme responsible for further catabolism.

The direct measurement of glucose metabolism with FDG also yields valuable information about tumor localization and quantitation (Fig. 4), and an exhaustive review article is available on the clinical aspects of FDG in oncology applications [54]. For tumor staging and assessment of treatment response, FDG and PET often distinguishes between non-tumorous masses from viable tumor [55], because of the increased glucose utilization in these malignant tumors. This transformation is often associated with downregulation of glucose-6-phosphate and the up-regulation of glucose transporters (especially GLUT-

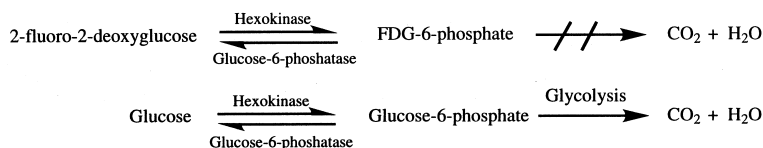


Fig. 3. The mechanism of uptake and trapping of 2-[ $^{18}\text{F}$ ]fluoro-2-deoxyglucose (FDG) in tumors.



Fig. 4. FDG image (anterior whole body). Image of a 38-year-old woman with a history of malignant melanoma. Multiple areas of increased FDG accumulation are present in the thorax, abdomen and pelvis. Images are reproduced with permission from the MIR-NM digital teaching file collection at Washington University School of Medicine.

1) and hexokinase. FDG is potentially useful in differentiating benign from malignant forms of stimulated osteoblastic activity because of the high metabolic activity of many types of aggressive tumors. FDG and PET also demonstrates the potential for non-invasive tumor staging because of its ability to detect lymph node metastases from breast and lung cancers, melanoma and head and neck carcinomas [56,57]. It is important to note that all cells metabolize glucose and therefore FDG is not tumor specific and can present a significant problem particularly after therapy when macrophages, which exhibit high uptake of FDG, replace tumor cells. Uptake can also be effected by blood sugar levels due to competition with glucose for membrane

transporters [58], but this can be dealt with by the clinician by fasting the patient 4–6 h prior to injection [54].

### 3.3. Amino acids

Although FDG has been a very useful tracer in the measurement of glucose metabolism in many types of tumors using PET, it is not necessarily the optimal tracer in all cases. For example, in neuro-oncology, tumor detection with FDG is often difficult due to the high basal metabolism in the brain [59–61]. Also, inflammatory cells have been reported to exhibit increased glucose metabolism, which may interfere with tumor imaging [62–64].

The *in vivo* study of other metabolic processes, such as the rates of protein, RNA or DNA synthesis, has been carried out to circumvent the problems associated with FDG. The rate of protein synthesis (PSR) in tumors can be quantified with positron-emitting amino acids or amino acid analogs, although it should be noted that the incorporation of an amino acid is the result of the synthesis of many different proteins. The first step in protein synthesis inside the cell is the enzymatic conversion of an L-amino acid into amino-acyl-tRNA by the enzyme amino-acyl RNA synthetase. Amino acids are also degraded by other pathways including decarboxylation, oxidation and transamination. Desirable properties of radiolabeled amino acids for quantifying the PSR include high blood-brain barrier permeability, rapid clearance and turnover, and favorable metabolic pathways. Using PET, it is not possible to discriminate between protein and non-protein bound radioactivity, therefore, the optimal amino acid should have minimal metabolism to non-proteins. A review of the use of amino acids for measurement of protein synthesis by PET has been reported [65].

Amino acids have been labeled with both  $^{11}\text{C}$  and  $^{18}\text{F}$  for PET imaging of tumors. Amino acids labeled in positions other than the carboxyl position have been found to undergo metabolism in more complicated processes than just protein formation, but are very useful nonetheless. Methionine has been labeled with  $^{11}\text{C}$  in the methyl and carboxyl position. L-[methyl- $^{11}\text{C}$ ]methionine was found to form a significant amount of non-protein bound metabolites *in*

*vivo*, making it difficult to accurately measure the PSR [66]; however, this agent has been of clinical value as a reliable marker of tumor tissue and can be a useful marker of amino acid transport [67]. For example, L-[methyl- $^{11}\text{C}$ ]methionine has been used in clinical studies to measure metabolic changes in breast cancer metastases in order to predict response to anticancer therapy [68]. It was found that an increase in uptake of L-[methyl- $^{11}\text{C}$ ]methionine 6–7 weeks after the beginning of therapy may be an indication of poor response. A comparative study with 3-[ $^{123}\text{I}$ ]iodo- $\alpha$ -methyltyrosine (SPECT) and L-[methyl- $^{11}\text{C}$ ]methionine (PET) showed that the two agents had comparable uptake and clearance in gliomas, indicating that amino acid transport can also be measured with gamma emitters [69].

L-[ $^{11}\text{C}$ ]tyrosine has been investigated extensively in the determination of PSR in tumors [70]. In a study of patients with brain tumors, it was found that prior to radiotherapy, gliomas were clearly visualized with L-[ $^{11}\text{C}$ ]tyrosine and PET, while after radiotherapy, all gliomas remained visible, with PSR values significantly higher than normal brain tissue. This indicated that the gliomas were still viable after radiotherapy. In patients with breast cancer, L-[ $^{11}\text{C}$ ]tyrosine was found to be able to distinguish between tumor and fibrocystic disease, whereas FDG did not [70].

#### 4. Receptor and transport-mediated radiopharmaceuticals

The over-expression of cell surface or nuclear receptors is the premise for receptor-based radiopharmaceuticals. To put in perspective the importance of this class of radiopharmaceuticals, in 1994 the Diagnostic Imaging Research Branch of the Division of Cancer Treatment of the National Cancer Institute held a workshop on 'Tumor Receptor Imaging' in Bethesda, MD. This workshop [71] covered many new advances in cancer biology involving hormone and growth factor receptors and certain biochemical changes that may serve as targets for tumor imaging.

In designing radiolabeled receptor-ligands, selectivity, low non-specific binding and incorporation of the radionuclide are three factors to consider. High

affinity for the receptor of interest and low affinity for other receptor systems improves selective tumor uptake. Designing agents with lower lipophilicity minimizes non-specific binding. For receptor-based radiopharmaceuticals, one of the most important considerations is that the radionuclide placement does not significantly decrease the receptor binding of the original ligand. Another important consideration is the stability of the radiolabeled-receptor ligand with respect to *in vivo* metabolism. Receptor ligands can be larger biomolecules such as peptides, or smaller organic molecules such as dopamine or folic acid. If a radiometal is used as the isotope of choice it is connected to these biomolecules *via* a bifunctional chelating agent (BFC), which consists of a chelate to complex the radiometal and a functional group for attachment to the biomolecule. These factors and others will be discussed in the following sections.

##### 4.1. $^{67}\text{Ga}$ - and $^{68}\text{Ga}$ -citrate

Cyclotron-produced  $^{67}\text{Ga}$  ( $t_{1/2} = 78$  h) decays by electron capture and has four principal gamma energies suitable for SPECT imaging: 93, 185, 300 and 394 keV. High spin Fe(III) and Ga(III), due to their similar electronic configuration ( $\text{Fe}^{3+} = 3d^5$ ,  $\text{Ga}^{3+} = 3d^{10}$ ), have many common properties, including ionic radii ( $\text{Fe}^{3+} = 0.49 \text{ \AA}$ ,  $\text{Ga}^{3+} = 0.47 \text{ \AA}$ ), ionization potential and coordination number. *In vivo*, gallium mimics iron.

$^{67}\text{Ga}$ -labeled citrate was first used in tumor imaging nearly 30 years ago [72], and a few years later researchers determined that the  $^{67}\text{Ga}$  was actually binding transferrin *in vivo* [73]. Today,  $^{67}\text{Ga}$ -citrate/transferrin remains a widely used radiopharmaceutical for the clinical diagnosis of certain types of neoplasms, such as Hodgkin's disease, lung cancer, non-Hodgkin's lymphoma, malignant melanoma and leukemia. In Fig. 5 an example of  $^{67}\text{Ga}$ -citrate uptake in malignant melanoma is shown. The mechanism of  $^{67}\text{Ga}$ -citrate/transferrin uptake into tumors has long been disputed. The current theory is that the  $^{67}\text{Ga}$ -transferrin complex binds to the transferrin receptor present on tumor cells, and is then incorporated into the cell by receptor-mediated endocytosis [74]. This theory was further examined by determin-

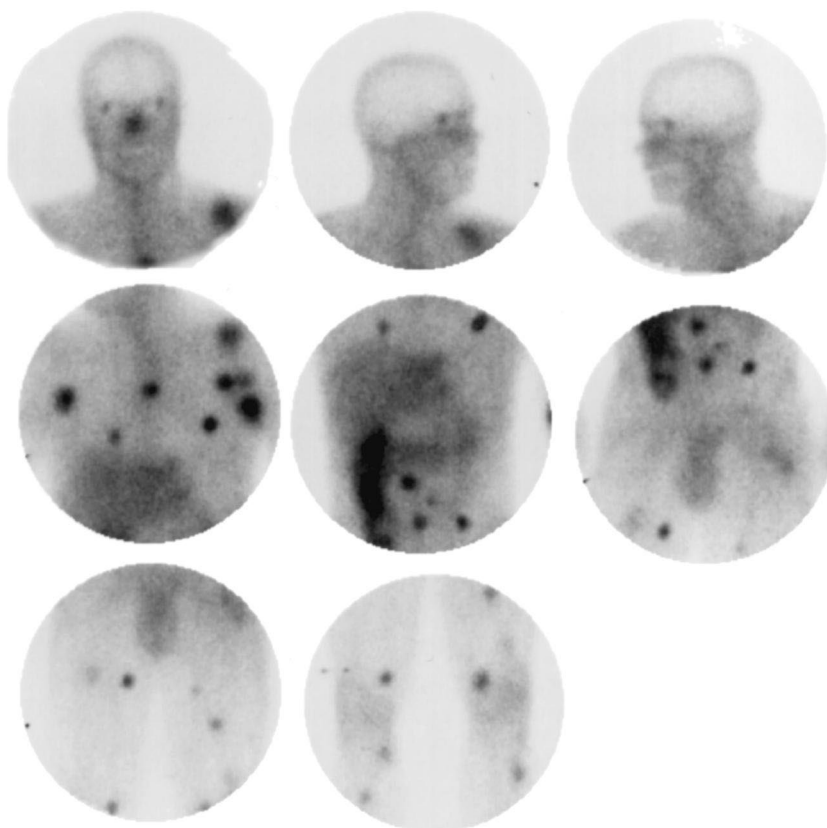


Fig. 5.  $^{67}\text{Ga}$ -citrate image (72 h post-injection). A  $^{67}\text{Ga}$ -citrate image of a 45-year-old man with a history of metastatic melanoma. The examination reveals foci of markedly increased activity throughout the upper extremities, axilla, chest, abdomen, pelvis, and lower extremities, bilaterally. Careful examination reveals the superficial nature of some of these lesions. In addition, abnormally increased activity is noted in the kidneys bilaterally. Images are reproduced with permission from the MIR-NM digital teaching file collection at Washington University School of Medicine.

ing the uptake of  $^{67}\text{Ga}$ -citrate in two cell lines: one that had no transferrin receptor, and one where the transferrin receptor was overexpressed [75] no return.

It was found that both transferrin-dependent and independent mechanisms were responsible for the uptake of  $^{67}\text{Ga}$  in these transfected cell lines.

$^{68}\text{Ga}$ -labeled citrate/transferrin has also been used in diagnostic imaging, but due to the much shorter half-life of  $^{68}\text{Ga}$  than  $^{67}\text{Ga}$ , the disease states studied are very different. For example,  $^{68}\text{Ga}$ -transferrin has been used to quantify pulmonary vascular permeability using PET [76], since  $^{68}\text{Ga}$ -transferrin is taken up in the lungs immediately after injection. PET allows quantification which is not possible with  $^{67}\text{Ga}$  and gamma scintigraphy; however, to date,

$^{68}\text{Ga}$ -citrate has not been used for tumor imaging with PET.

#### 4.2. MIBG

Meta-iodobenzylguanadine (MIBG), a structural analog of guanidine (Fig. 6), is an adrenergic blocking agent [77]. Like guanidine, MIBG enters the adrenergic tissue and is concentrated in the catecholamine storage vesicles of adrenergic nerve endings and the adrenal medulla. MIBG accumulates in tumors of the neural crest tissue and adrenal medulla such as pheochromocytomas, non-functioning paragangliomas, carcinoid tumors, neuroblastomas and certain neuroendocrine tumors. MIBG has also been used for imaging the medullary carcinoma

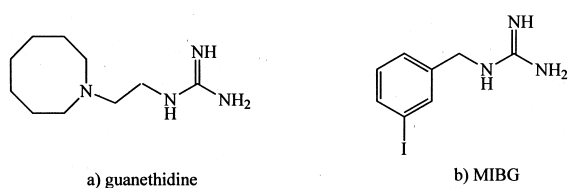


Fig. 6. Structure of guanethidine (a) and its analog, MIBG (b) that is used for imaging of adrenal tumors and neuroblastoma.

of the thyroid [78], retinoblastoma [79] melanoma and bronchial cell carcinoma [80].

MIBG is similar in chemical structure to norepinephrine, a neurotransmitter-hormone, and physiologically distributes similarly. The uptake of MIBG in normal and tumorous adrenergic tissues appears to involve the re-uptake mechanism of norepinephrine that does not bind to receptors in the membrane of the post synaptic effector cell [81]. Two systems have been identified for MIBG uptake in adrenergic cells. Uptake system I, is specific for catecholamines, is saturable, sodium, energy and temperature dependent and has a high affinity for MIBG [82]. This is the predominant mode involved in diagnostic imaging [83–85]. Uptake system II is non-saturable, sodium or energy independent, temperature dependent, low affinity for MIBG and predominates at high concentrations of MIBG [82–85]. Upon entering the cytoplasm, MIBG and other catecholamines are concentrated in adrenergic storage vesicles by an energy dependent proton pump [81,86].

Isotopes of iodine used to label MIBG for diagnostic imaging and radiotherapy are listed in Tables 1 and 2. The advantages of labeling with iodine are its relative ease, the retention of the molecule's overall distribution characteristics, and convenient half lives that allow sufficient time between synthesis, injection and imaging. Since only a small fraction of circulating blood passes through adrenergic tissue, a relatively long period of time is required for the tracer to accumulate in the target tissue and clear from the blood and non-target tissues.

Imaging with MIBG can localize sites of neuroblastoma not detectable with other imaging modalities [87]. Accurate detection and localization is essential as surgical resection is the most effective treatment for localized neuroblastoma [88–91]. If the

disease has metastasized to the lymph nodes or if the primary tumor is located in a site with limited access it is difficult for the surgeon to achieve complete resection. A study into using  $^{123}\text{I}$  and  $^{125}\text{I}$  labeled MIBG demonstrated the feasibility of using MIBG as a radioguide to ensure complete resection of neuroblastoma in children. Improved image quality and detection has been achieved by using SPECT in combination with  $^{123}\text{I}$ . Metastases not observable using  $^{131}\text{I}$  MIBG were detected with SPECT and  $^{123}\text{I}$  imaging [92].

#### 4.3. Somatostatin analogs

Some of the first peptide-based tumor receptor imaging agents were radiolabeled analogs of the hormone somatostatin. Somatostatin (Fig. 7) is a 14-amino acid peptide involved in the regulation and release of a number of hormones, including growth hormone, thyroid-stimulating hormone and prolactin. Somatostatin receptors (SSRs), found on the cell surface, occur in a number of different normal organ systems including the central nervous system, the gastrointestinal tract, and the exocrine and endocrine pancreas [93–95]. A large number of human tumors are also SSR-positive [96]. Somatostatin has a very short biological half-life, but analogs such as octreotide have much longer residence times [97].

Octreotide, an 8-amino acid somatostatin analog, has been labeled with  $^{111}\text{In}$  using DTPA [98,99] (Fig. 7) and is approved for human use in the U.S.A. and Europe as a diagnostic imaging agent for neuroendocrine tumors [100,101]. This agent shows low nanomolar affinities for SSR in neuroendocrine tumors [102], and > 80% of  $^{111}\text{In}$ -DTPA-octreotide clears rapidly through the kidneys intact [100] (Fig.

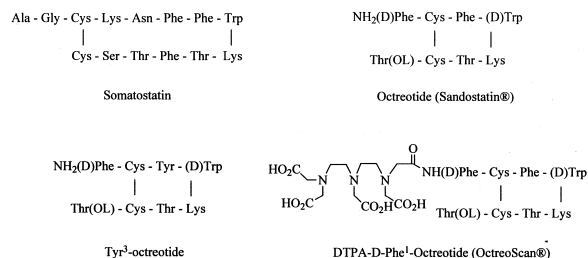


Fig. 7. Somatostatin and analogs that are used in the imaging of neuroendocrine tumors.



doocrine cancer. The uptake kinetics of 2-[ $^{18}\text{F}$ ]fluoropropionyl-(D)phe<sup>1</sup>-octreotide were determined by PET and *ex vivo* biodistribution and compared to  $^{67}\text{Ga}$ -DFO-octreotide [105]. This  $^{18}\text{F}$ -labeled octreotide analog accumulated rapidly in SSR-positive tumors in rats, but it cleared substantially by 2 h post-injection. Conversely,  $^{67}\text{Ga}$ -DFO-octreotide was retained by the tumor. 2-[ $^{18}\text{F}$ ]fluoropropionyl-(D)phe<sup>1</sup>-octreotide cleared through the hepatobiliary system, in contrast to  $^{67}\text{Ga}$ -DFO-octreotide, which cleared through the kidneys. At the time of this writing, no  $^{18}\text{F}$ -labeled octreotide analogs have suitable tumor uptake and clearance characteristics for PET imaging of SSR positive tumors in humans.

Octreotide has been conjugated to the BFCs CPTA and TETA (Fig. 9), for labeling with  $^{64}\text{Cu}$  [102]. CPTA, a derivative of cyclam, forms Cu(II) complexes having a +1 charge, whereas the Cu-TETA complex has a -1 charge.  $^{64}\text{Cu}$ -CPTA-octreotide and  $^{64}\text{Cu}$ -TETA-octreotide showed high affinity for the SSR both *in vitro* and *in vivo*, but their biological clearances were very different. The  $^{64}\text{Cu}$ -CPTA conjugate cleared almost exclusively and very slowly through the liver.  $^{64}\text{Cu}$ -TETA-octreotide cleared primarily through the kidneys, with very low liver accumulation. These results demonstrate that the BFC has a major impact on the biological behavior of radiometal-BFC-biomolecule conjugates.  $^{64}\text{Cu}$ -TETA-octreotide is currently being evaluated as a PET imaging agent for neuroendocrine tumors [106]. Preliminary results showed that  $^{64}\text{Cu}$ -TETA-octreotide and PET detected even more SSR positive lesions than the currently used agent,  $^{111}\text{In}$ -DTPA-octreotide and gamma scintigraphy.

Octreotide analogs have also been labeled with  $^{86}\text{Y}$  for PET imaging prior to radiotherapy with  $^{90}\text{Y}$  [105,107–110].  $^{90}\text{Y}$ -DTPA was unstable *in vivo*, resulting in high bone uptake [105,107], but  $^{90}\text{Y}$ -DOTA was found to be very stable.  $^{86/90}\text{Y}$ -DOTA-Tyr<sup>3</sup>-octreotide has demonstrated high target uptake and rapid renal clearance [108,109]. Clinical trials for PET imaging and radiotherapy using  $^{86}\text{Y}$ - and  $^{90}\text{Y}$ -labeled DOTA-octreotide are imminent [108,109].

Technetium and rhenium have been complexed to somatostatin analogs *via* chelates formed from peptides containing the amino acids glycine, cysteine

and lysine [111]. Two of the peptides evaluated *in vitro* by Pearson, et al.,  $^{99\text{m}}\text{Tc}$ -labeled P587 and P829 [111], were studied further in animal models [112]. These  $^{99\text{m}}\text{Tc}$ -labeled peptides both have high binding affinity to the SSR in tumor-bearing rats and favorable clearance characteristics. Clinical investigations are ongoing [113].

Somatostatin analogs, based on alterations in the structure of octreotide, where Tyr(Y) is substituted for Phe(F) in the 3-position, and/or the C-terminal alcohol is replaced with a carboxylate, demonstrated increased affinity for SSR and increased uptake in SSR<sup>+</sup> tissues *in vivo*. These substitutions have been made for  $^{111}\text{In}$ -DTPA,  $^{111}\text{In}$ -DOTA and  $^{64}\text{Cu}$ -TETA conjugates and have resulted in significantly higher SSR<sup>+</sup> tissue uptake compared to  $^{111}\text{In}$ -DTPA-octreotide [114,115] and  $^{64}\text{Cu}$ -TETA-octreotide [116].

#### 4.4. Steroid receptor ligands

Unlike many cell surface receptors targeted by radiopharmaceuticals, receptors for steroid hormones are nuclear proteins and interact at specific sites in chromatin. Biological action occurs when the steroid penetrates the cell membrane and forms a complex with the receptor that then associates tightly with the specific regulatory binding sites in the chromatin. There are typically about 10,000 steroid receptors per prostate or breast cancer tumor cell, and the affinities of these nuclear receptors for their ligands are generally in the subnanomolar-to-nanomolar range [117].

During the early 1980's, steroid ligands labeled with radiohalogens were evaluated as imaging agents for hormone receptor-positive tumors [118–122]. In the estradiol molecule, bromine or iodine were found to be tolerated only at the 16 $\alpha$ -position; however, fluorine, a much smaller halogen, is well tolerated at every substituent position and causes no decrease in binding affinity or increase in non-specific binding. Of the  $^{18}\text{F}$ -labeled estrogen receptor ligands evaluated, 16 $\beta$ -fluoro-11 $\beta$ -methoxy-17 $\alpha$ -ethynyl estradiol ( $\beta\text{FMOX}$ ) (Fig. 10) had the most favorable uptake in the estrogen receptors of the immature rat uterus [123]. However, 16 $\alpha$ -[ $^{18}\text{F}$ ]fluoro-17 $\beta$ -estradiol (FES) (Fig. 10), one of the initial fluorinated estrogen analogs evaluated, had the most favorable biodistribution in humans; [124] (F. Dehdashti, unpublished

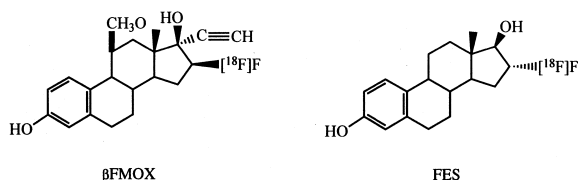


Fig. 10. Estrogen receptor ligands. Structures of 16 $\beta$ -fluoro-11 $\beta$ -methoxy-17 $\alpha$ -ethynyl estradiol ( $\beta$ FMOX) and 16 $\alpha$ -[ $^{18}$ F]fluoro-17 $\beta$ -estradiol (FES).

results). This difference may be because  $\beta$ FMOX was designed to have a low affinity for sex hormone binding globulin (SHBG), because it was thought that this protein would decrease the available steroid capable of binding estrogen receptors [125]. A more recent model of SHBG and steroid receptor ligands suggests that the protein actually transports the steroid to its receptor [126]. A review by Jonson and Welch has further discussion of SHBG and steroid receptor ligand interactions [127].

Androgen receptors are typically found in prostate cancer, and an androgen receptor-based radiopharmaceutical may be useful in imaging the disease. Several  $^{18}$ F-labeled androgen receptor ligands (16 $\beta$ - $^{18}$ F-substituted testosterone, 5 $\alpha$ -dihydrotestosterone and mibolerone, 16 $\alpha$ - and 16 $\beta$ - $^{18}$ F-7 $\alpha$ -methyl-19-nortestosterone, 20-[ $^{18}$ F]-fluoroR1881 (metribolone) and 20-[ $^{18}$ F]-fluoromibolerone) have been synthesized and evaluated in male rats [128,129]. Of these, three agents were selected for imaging in a non-human primate model: 16 $\beta$ -[ $^{18}$ F]fluoro-5 $\alpha$ -dihydrotestosterone (16 $\beta$ -[ $^{18}$ F]FDHT), 16 $\beta$ -[ $^{18}$ F]fluoromibolerone, and 20-[ $^{18}$ F]-fluoromibolerone [130]. A steroid-SHBG effect has also been observed with these androgens. 16 $\beta$ -[ $^{18}$ F]FDHT (Fig. 11) showed a 37-fold greater

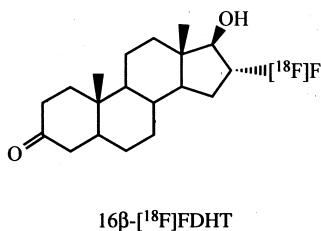


Fig. 11. Structure of 16 $\beta$ -[ $^{18}$ F]fluoro-5 $\alpha$ -dihydrotestosterone (16 $\beta$ -[ $^{18}$ F]FDHT) used for imaging androgen receptors in prostate cancer.

prostate:bone ratio in baboons compared to rats, and this agent is currently being evaluated as a prostate cancer imaging agent in humans [131].

## 5. Monitoring cancer therapy with radiopharmaceuticals

### 5.1. Monitoring hormonal therapy with FES

An important aspect of receptor-based imaging agents is their use in the monitoring of conventional or chemotherapy regimes in cancer patients. In patients with primary and metastatic breast cancer, data obtained from PET imaging after FES administration correlates with tumor estrogen receptor status determined *in vitro* [132]. Comparison studies showed that FDG was more sensitive than FES in staging breast cancer, and that patients who are estrogen receptor positive (ER+) by *in vitro* assays, but FES negative, may be less likely to respond to hormone therapy [133].

Tamoxifen therapy in breast cancer patients frequently is accompanied by a 'flare' reaction, defined as pain and swelling following initiation of therapy. Clinically, it may be difficult to distinguish between a flare reaction and disease progression. Further evaluation using FDG and FES in breast cancer patients undergoing tamoxifen therapy was carried out to determine if increased FDG uptake after initiating tamoxifen therapy ('metabolic flare') predicted a hormonally responsive breast cancer [134]. There was a significant correlation between increased tumor uptake of FDG and greater blockade of FES 7–10 days after initiation of tamoxifen therapy in patients who responded to the hormonal therapy than in non-responders.

### 5.2. Multi-drug resistance

A major cause of failure in the treatment of cancer is the development of multi-drug resistance (MDR). MDR is a condition in which the tumor acquires resistance to a structurally and functionally diverse group of compounds following administration of a single chemotherapeutic agent. The resistance correlates to the overexpression of a family of related mammalian MDR and multidrug resistance-associ-

ated (MRP) genes which code for transporters that pump drugs out of the cell [135–138]. The best characterized of these transporters is P-glycoprotein (Pgp), a transmembrane protein ( $M_r = 170\,000$ ) expressed on the plasma membrane of tumor cells [139,140]. Pgp is an ATP dependent efflux pump that renders resistance by transporting chemotherapeutic agents out of the cell.

MDR reversal or modulator agents are drugs that could be co-administered with the chemotherapeutic drugs to block or inhibit these transporters and thereby enhance accumulation of chemotherapeutic drugs. The first generation of modulators, cyclosporin A and verapamil, were successful experimentally in inhibiting MDR mediated by Pgp. When used clinically, however, these agents proved to be ineffective as their toxic side effects occurred before reversal of MDR was achieved [141]. Research has since focused on developing agents that inhibit Pgp at concentrations that will not induce cytotoxic or pharmacological side effects. Although these drugs tend to be quite diverse chemically, many are lipophilic and positively charged at neutral pH [142].

Immunohistochemical techniques to characterize Pgp expression in human tumors [143–149] require tissue biopsies, are labor intensive and can be unreliable due to tumor heterogeneity [137,150]. Based on these limitations and the need for an *in vivo* assay to evaluate newly developed MDR reversal agents, an imaging agent was sought. As substrates of Pgp tend to be lipophilic and monocationic at physiological pH, the same requirements common to agents developed for myocardial imaging, the possibility was raised that myocardial imaging agents might be suitable substrates for Pgp.

The first myocardial agent evaluated as a possible substrate for Pgp was  $^{99m}\text{Tc}$ -hexakis(2-methoxy-isobutylisonitrile) (sestamibi) (Fig. 12).  $^{99m}\text{Tc}$ -sestamibi consists of technetium in the 1+ oxidation state bound to six alkyl isonitrile groups in an octahedral geometry [151], and the complex is extremely stable *in vivo*.  $^{99m}\text{Tc}$ -sestamibi accumulation in mitochondria is driven by membrane potential. The initial distribution of  $^{99m}\text{Tc}$ -sestamibi into mitochondrial rich tissues accounts for its accumulation in the heart, kidney, liver, skeletal muscle and tumors *in vivo*.  $^{99m}\text{Tc}$ -sestamibi is a substrate of Pgp [152–156]; a three fold difference is observed between

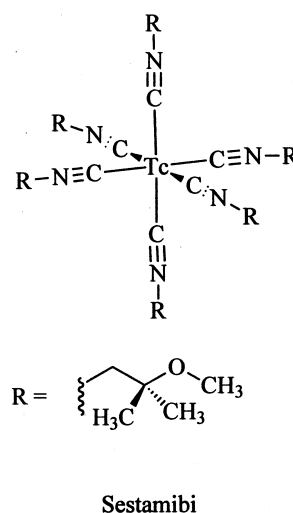


Fig. 12.  $^{99m}\text{Tc}$ -sestamibi: Imaging agents for multi-drug resistance (MDR) in tumors.

MDR expressing and non-expressing tissues. Clinical evaluation of  $^{99m}\text{Tc}$ -sestamibi demonstrated efficient functional imaging of Pgp expression in breast cancer patients [157] and patients with refractory cancer [158].

### 5.3. Imaging of tumor hypoxia

A major problem faced in treating cancer is the resistance of tumors to treatment. Besides MDR, another cause of tumor resistance is the development of hypoxic regions (areas of low oxygen tension) within tumors. Hypoxic regions have been shown to be resistant to traditional chemotherapy [159–161] and radiotherapy [162,163]. Compounds known as hypoxic cell sensitizers have been developed that render these regions more sensitive to radiation. Methods exist for measuring hypoxia, however a non-invasive diagnostic test would be useful for clinical applications [164,165]. Radiopharmaceuticals selectively retained by these hypoxic regions would provide a non-invasive technique and would be of benefit in determining the course and success of treatment.

The first radiopharmaceutical agents for hypoxia were based on nitroimidazoles, a class of hypoxic cell sensitizing agents. After diffusing into a cell, nitroimidazoles undergo a one-electron reduction in

viable cells, forming an anionic radical, that upon reoxidation in normal cells diffuses out of the cell. In hypoxic cells the nitroimidazoles are further reduced to more reactive species that bind to cell components [165]. Analogs of nitroimidazoles have been labeled with  $^{18}\text{F}$  for PET imaging and  $^{123}\text{I}$  for SPECT imaging. The fluorinated analog, [ $^{18}\text{F}$ ]-fluoromisonidazole (FMISO) (Fig. 13) is retained in hypoxic tissue in cerebral ischemia, [166,167] myocardial infarction [168,169] and tumors [170]. Although the differences between hypoxic tissue and normal tissue are seen by PET and SPECT with these analogs, they suffer from low cellular uptake and slow normal tissue clearance requiring long periods of time between injection and imaging [168,169,171].

Chelates coordinated to 2-nitroimidazole groups have been labeled with  $^{99\text{m}}\text{Tc}$  [172–175]. These complexes exhibited specific retention in hypoxic tissue in models of myocardial ischemia [173,176,177] and in tumors [178]. Bristol–Myers Squibb developed several  $^{99\text{m}}\text{Tc}$  labeled 2-nitroimidazole complexes by coordinating ligands that form neutral Tc complexes to nitroimidazole groups known to be selective for hypoxic tissue. The first such compounds were the neutral  $^{99\text{m}}\text{Tc}$ -BATO complex conjugated to either a 2- or 4-nitroimidazole moiety [172]. The reduction of the nitroimidazole groups of these compounds was found to be more difficult to reduce than misonidazole [172,179]. This was considered a problem since the selective trapping in hypoxic tissue is due to the reduction of the nitroimidazoles. Another agent was developed that incorporated technetium(V) propylene amine oxide (Tc-PnAO) to 2-nitroimidazole (BMS-181321); this was shown to be selective for hypoxic tissue. An

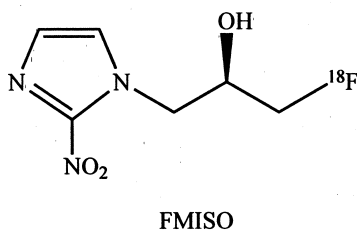


Fig. 13. Structure of [ $^{18}\text{F}$ ]-fluoromisonidazole (FMISO), an analog of 2-nitroimidazole that is used to image hypoxia in tumors.

improved compound (DM5-194796) has since been described [180].

In certain cases the technetium core complexes without the nitroimidazole groups have even greater hypoxia selectivity than the nitroimidazole containing complexes [181]. Based on this finding the compound,  $^{99\text{m}}\text{Tc}$ -HL91, which does not contain a nitroimidazole group and is similar in structure to BMS-181321, was evaluated for its hypoxic selectivity. It demonstrated increased uptake in hypoxic and low flow ischemic myocardium [182], and in a preliminary study uptake in human tumors seemed to be attributable to the presence of hypoxic tissue [165]. The major disadvantage of this agent is that imaging times of up to 4 h are required for optimal contrast [183].

Fujibayashi and co-workers [184,185] have shown that a copper complex, Cu(II)-diacetyl-bis( $N^4$ -methylthiosemicarbazone) (Cu-ATSM) (Fig. 14), is retained in ischemic tissue but diffuses out of normoxic tissue. This complex is in a class of copper bis(thiosemicarbazones) which have been evaluated *in vitro* and display uptake that is either non-hypoxia selective (e.g. Cu-PTSM) to hypoxic selective [186]. The variety of copper radionuclides available allows the potential of multiple isotope studies utilizing Cu-ATSM or in conjunction with a blood flow tracer such as Cu-PTSM. Studies conducted using the Langendorff isolated perfused rat heart model, in which oxygen concentration can be controlled, showed that specific retention of Cu-ATSM is due to oxygen depletion [187]. It has also been shown that

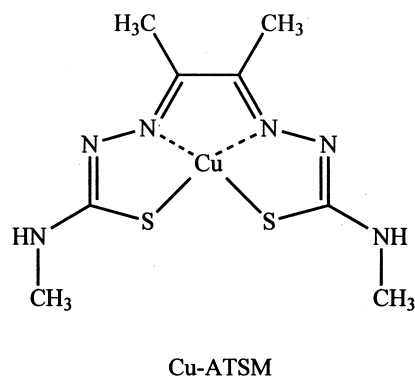


Fig. 14. Structure of Cu(II)-diacetyl-bis( $N^4$ -methylthiosemicarbazone) (Cu-ATSM).

$^{60}\text{Cu}(\text{ATSM})$  can delineate hypoxic tissue in tumors *in vivo* [188].  $\text{Cu-ATSM}$  differs from the blood flow agent  $\text{Cu-PTSM}$  by the addition of a single methyl group on the ligand backbone, which results in a 100 mV lowering of the reduction potential of  $\text{Cu-ATSM}$ . In the case of  $\text{Cu-PTSM}$ ,  $\text{Cu(II)}$  is reduced to  $\text{Cu(I)}$  by the normal electron transport chain of mitochondria in both normoxic and hypoxic tissue (Fig. 1), whereas with  $\text{Cu-ATSM}$ ,  $\text{Cu(II)}$  is only reduced by oxygen depleted mitochondria in hypoxic tissue [185,189,190]. The reduction of  $\text{Cu-ATSM}$  requires both abnormally high NADH concentrations and intact Complex I system mitochondrial electron transport chain. Thus, the retention of  $\text{Cu-ATSM}$  indicates the presence of intact mitochondria, but disturbed electron flow (namely high NADH) caused by depletion of the final electron acceptor, oxygen.  $\text{Cu-ATSM}$  with its lower redox potential is not reduced in normoxic tissue and therefore quickly washes out. In hypoxic tissues, the  $\text{Cu(II)}$  of  $\text{Cu-ATSM}$  is quickly and irreversibly reduced to  $\text{Cu(I)}$  and retained. The higher redox potential of  $\text{Cu-PTSM}$  allows it to be reduced in both normoxic and hypoxic tissue and therefore retained in both.

## 6. Summary and conclusion

Over the past few decades the diagnosis of disease with radiopharmaceuticals has progressed from rudimentary radioactive small molecule tracers to targeting molecules based upon defined biological and chemical processes. With the availability of sophisticated imaging modalities and radionuclides the clinician has available techniques for the non-invasive diagnosis of cancer as well as the means to accurately monitor the efficacy of therapeutic treatments. In this review we have discussed three such available methods; the utilization of metabolic, transport and receptor-mediated processes to deliver agents for cancer diagnosis.

It is now possible to identify the presence of cancer (e.g. FDG), the type of tumor with specific receptor based drugs (e.g. androgen, estrogen, somatostatin receptor positive cancer) and to monitor the effectiveness of treatment (e.g. the existence of hypoxia). With the advances in drug design and the large numbers of tumor types, the opportunity now

exists for the scientist to look at a particular disease and to identify what discriminates it from healthy tissue. With this knowledge at hand and the myriad of tumor targeting mechanisms available, radiopharmaceuticals can be designed accurately to target a particular type of cancer.

## 7. Glossary

ATSM	diacetyl-bis( $N^4$ -methylthiosemicarbazone)
$\beta\text{FMOX}$	16 $\beta$ -fluoro-11 $\beta$ -methoxy-17 $\alpha$ -ethynyl estradiol
BFC	bifunctional chelator
BMS-181321	oxo((3,3,9-tetramethyl-1-(2-nitro-1H-imidazol-1-yl)-4,8-diazaundecane-2,10-dione dioximate)(3-)- $N,N',N'',N'''$ )-technetium(V)
CPTA	4-[(1,4,8,11-tetraazacyclotetradec-1-yl)methyl]benzoic acid
DFO	desferrioxamine-B
DMAD	dimethyleneaminomethylene diphosphate
DTPA	diethylenetetraaminepentaacetic acid
EDTA	ethylenediaminetetraacetic acid
FES	16 $\alpha$ -[ $^{18}\text{F}$ ]fluoro-17 $\beta$ -estradiol
FDG	2-[ $^{18}\text{F}$ ]fluoro-2-deoxyglucose
16 $\beta$ -[ $^{18}\text{F}$ ]FDHT	16 $\beta$ -[ $^{18}\text{F}$ ]fluoro-5 $\alpha$ -dihydro-testosterone
FMISO	[ $^{18}\text{F}$ ]-fluoromisonidazole
[ $^{18}\text{F}$ ]-FU	$^{18}\text{F}$ -labeled fluorouracil
h	hours
HEDP	1-hydroxyethylidene diphosphate
HMDP	hydroxymethylene diphosphate
HSA	human serum albumin
keV	kilo-electron volts ( $10^3$ )
mAb	monoclonal antibody
MDP	methylene diphosphate
MDR	multi-drug resistance
MeV	mega-electron volts ( $10^6$ )
PET	positron emission tomography
PTSM	pyruvaldehyde-bis( $N^4$ -methylthiosemicarbazone)
sestamibi	2-methoxyisobutaneisonitrile

SHBG	sex hormone binding globulin
SPECT	single photon emission computed tomography
SSR	somatostatin-receptor
TETA	1,4,8,11-tetraazacyclotetradecane-1,4,8,11-tetraacetic acid

## Acknowledgements

The authors wish to thank Joanna B. Downer for proofreading this manuscript and the financial support from the Department of Energy and the National Institutes of Health.

## References

- [1] G. Subramanian, B.A. Rodes, J.F. Cooper, V.D. Sodd, *Radiopharmaceuticals*, The Society of Nuclear Medicine, New York, 1975.
- [2] B.A. Rhodes, B.Y. Craft, *Basics of Pharmacy*, C.V. Mosby Co., St. Louis, MO, 1978.
- [3] R.J. Callahan, F.P. Castronovo, Development of technetium-99m labeled 1-hydroxy-ethylidene-1,1-disodium phosphonate for skeletal imaging, *Am. J. Hosp. Pharm.* 30 (1973) 614–617.
- [4] Y. Yano, J. McRae, D.C. Van Dyke, H.O. Anger, Technetium-99m-labeled stannous ethane-1-hydroxy-1,1-diphosphonate: a new bone scanning agent, *J. Nucl. Med.* 14 (1973) 73–78.
- [5] J.W. Keyes, J. Carey, D. Moses, W. Beierwaites, *Manual of Nuclear Medicine Procedures*, CRC Press, Cleveland, Ohio, 1973.
- [6] N.D. Heindel, H.D. Bums, T. Honda, L.W. Brady, *The Chemistry of Radiopharmaceuticals*, Masson, New York, 1978.
- [7] R.P. Beaney, Positron emission tomography in the study of human tumors, *Sem. Nucl. Med.* 14 (1984) 324–341.
- [8] A.A. Lammertsmaa, T. Jones, Low oxygen extraction fraction in tumors measured with the oxygen-15 steady state technique: effect of tissue heterogeneity, *Br. J. Radiol.* 65 (1992) 697–700.
- [9] K. Mineura, T. Sasajima, M. Kowada, T. Ogawa, J. Hatazawa, K. Uemura, Long-term positron emission tomography evaluation of slowly progressive gliomas, *Eur. J. Cancer* 32A (1996) 1257–1260.
- [10] P. Herscovitch, J. Markham, M.E. Raiche, Brain blood flow measured with intravenous  $H_2^{15}O$ , *J. Nucl. Med.* 24 (1983) 782–789.
- [11] A. Dimitrakopoulou, L.G. Strauss, J.H. Clorius, H. Ostertag, P. Schlag, M. Heim, F. Oberdorfer, F. Helus, U. Haberkom, G. van Kaick, Studies with positron emission tomography after systemic administration of fluorine-18-uracil in patients with liver metastases from colorectal carcinoma, *J. Nucl. Med.* 34 (1993) 1075–1081.
- [12] A. Dimitrakopoulou-Strauss, L.G. Strauss, P. Schlag, P. Hohenberger, G. Imgartinger, F. Oberkorfer, J. Doll, G. van Kaick, Intravenous and intra-arterial oxygen-15-labeled water and fluorine-18-labeled fluorouracil in patients with liver metastases from colorectal carcinoma, *J. Nucl. Med.* 39 (1998) 465–473.
- [13] T. Nariai, M. Senda, K. Ishii, T. Maehara, S. Wakabayashi, H. Toyama, K. Ishiwata, K. Hirakawa, Three-dimensional imaging of cortical structure, function and glioma for tumor resection, *J. Nucl. Med.* 38 (1997) 1563–1568.
- [14] H.G. Petering, H.H. Buskirk, G.E. Underwood, Antitumor action of 2-oxo-3-ethoxybutyraldehyde bis(thiosemicarbazone) and similar compounds, *Cancer Res.* 24 (1964) 367–372.
- [15] D.H. Petering, Physicochemical properties of the anti-tumor agent 3-ethoxy-2-oxobutyraldehyde bis-(thiosemicarbazonato)-copper(II), *Bioinorg. Chem.* 1 (1972) 255–271.
- [16] D.H. Petering, The reaction of 3-Ethoxy-2-oxobutyraldehyde bis(thiosemicarbazonato)copper(II) with thiols, *Bioinorg. Chem.* 1 (1972) 273–288.
- [17] Y. Fujibayashi, K. Wada, H. Taniuchi, Y. Yonekura, J. Konishi, A. Yokoyama, Mitochondria-selective reduction of  $^{62}Cu$ -pyruvaldehyde-bis( $N^4$ -methylthiosemicarbazone) ( $^{62}Cu$ -PTSM) in the murine brain; a novel radiopharmaceutical for brain positron emission tomography (PET) imaging, *Biol. Pharm. Bull.* 16 (1993) 146–149.
- [18] M.A. Green, C.J. Mathias, M.J. Welch, A.H. McGuire, D. Perry, F. Fernandez-Rubio, J.S. Perlmutter, M.E. Raichie, S.R. Bergmann, Copper-62-labeled pyruvaldehyde bis( $N^4$ -methylthiosemicarbazonato)copper(II): Synthesis and evaluation as a positron emission tomography tracer for cerebral and myocardial perfusion, *J. Nucl. Med.* 31 (1990) 1989–1996.
- [19] J.L. Lacy, S.C. Chien, J.K. Lim, C.J. Mathias, M.A. Green, Modular automated Zn-62/Cu-62 PET radiopharmaceutical generator, *J. Nucl. Med.* 36 (1995) 49.
- [20] K. Matsumoto, Y. Fujibayashi, Y. Yonekura, Application of the new zinc-62/copper-62 generator: An effective labeling method for  $^{62}Cu$ -PTSM, *Nucl. Med. Biol.* 19 (1992) 39–44.
- [21] D.W. McCarthy, R.E. Shefer, R.E. Klinkowstein, L.A. Bass, W.H. Margeneau, C.S. Cutler, C.J. Anderson, M.J. Welch, Efficient production of high specific activity  $^{64}Cu$  using a biomedical cyclotron, *Nucl. Med. Biol.* 24 (1997) 35–43.
- [22] L.A. Bass, D.W. McCarthy, L.A. Jones, P.D. Cutler, R.E. Shefer, R.E. Klinkowstein, S.W. Schwarz, C.S. Cutler, J.S. Lewis, C.J. Anderson, M.J. Welch, High purity production and potential applications of copper-60 and copper-61, *J. Label Comp. Radiopharm.* 40 (1997) 325–327.
- [23] P.J. Blower, J.S. Lewis, J. Zweit, Copper radionuclides and radiopharmaceuticals in nuclear medicine, *Nucl. Med. Biol.* 23 (1996) 957–980.
- [24] M.A. Green, A potential copper radiopharmaceutical for imaging the heart and brain: copper-labeled pyruvaldehyde bis( $N^4$ -methylthiosemicarbazone), *Nucl. Med. Biol.* 14 (1987) 59–61.

- [25] E.K. John, M.A. Green, Structure-activity relationships for metal-labeled blood flow tracers: comparison of ketoaldehyde bis(thiosemicarbazonato)copper(II) derivatives, *J. Med. Chem.* 33 (1990) 1764–1770.
- [26] M.E. Shelton, M.A. Green, C.J. Mathias, M.J. Welch, S.R. Bergmann, Assessment of regional myocardial and renal blood flow using copper-PTSM and positron emission tomography, *Circulation* 82 (1990) 990–997.
- [27] C.J. Mathias, M.J. Welch, D.J. Perry, A.H. McGuire, X. Zhu, J.M. Connett, M.A. Green, Investigation of copper-PTSM as a PET tracer for tumor blood flow, *Nucl. Med. Biol.* 18 (1991) 807–811.
- [28] J.L. Ritchie, G.W. Hamilton, Thallium-201 myocardial imaging, in: J.L. Ritchie, G.W. Hamilton, F.G. Wackers (Eds.), *Biological Properties of Thallium*, Raven Press, New York, 1978.
- [29] P.J. Gehring, P.B. Hammond, The interrelationship between thallium and potassium in animals, *J. Pharmacol. Exp. Ther.* 55 (1967) 187–201.
- [30] A.M. Sehweil, J.H. McKillop, R. Milroy, R. Wilson, H.M. Abdel-Dayem, Y.T. Omar, Mechanism of thallium-201 uptake in tumors, *Eur. J. Nucl. Med.* 15 (1989) 376–379.
- [31] A.D. Waxman, L. Ramana, J. Said, Thallium scintigraphy in lymphoma: relationship to gallium-67 (abstract), *J. Nucl. Med.* 30(S) (1989) 915.
- [32] M.J. Sessler, P. Geck, F.D. Maul, G. Hor, D.L. Munz, New aspects of cellular thallium uptake:  $Tl^+ - Na^+ - 2Cl^-$  cotransport is the central mechanism of ion uptake, *Nuklearmedizin* 25 (1986) 24–27.
- [33] H.S. Winchell, Mechanisms for localization of radiopharmaceuticals in neoplasms, *Sem. Nucl. Med.* 6 (1976) 371–378.
- [34] T. Brismar, V.P. Collins, M. Kesselberg, Thallium-201 uptake relates to membrane potential and potassium permeability in human glioma cells, *Brain Res.* 500 (1989) 30–36.
- [35] K.T. Black, R.A. Hawkins, K.T. Kim, Thallium-201 (SPECT): A quantitative technique to distinguish low grade from malignant brain tumors, *J. Neurosurgery* 71 (1989) 342–346.
- [36] K.T. Kim, K.L. Black, D. Marciano, J.C. Mazziota, B.H. Guze, S. Grafton, R.A. Hawkins, D.P. Becker, Thallium-201 SPECT imaging of brain tumors: methods and results, *J. Nucl. Med.* 31 (1990) 965–969.
- [37] H. Macapinlac, C.I. Caluser, J. Finlay et al, Correlation of Tl-201 brain SPECT with MR imaging in the post therapy evaluation of patients with primary malignant brain tumors, *Radiology* 181 (1991) 129.
- [38] H. Macapinlac, J. Finlay, C. Caluser, S. Yeh, A. Scott, R. Delapaz, K. Lindsley, R. Finn, A. Muraki, S. Larson, H. Abdel-Dayem, Comparison of Tl-201 SPECT and F-18 FDG PET imaging with MRI (Gd-DTPA) in the evaluation of recurrent and supratentorial and infratentorial brain tumors, *J. Nucl. Med.* 33 (1992) 862.
- [39] V.W. Lee, AIDS Related Kaposi Sarcoma, *AJR Am. J. Roentgenol.* (1988) 1233–1235.
- [40] M. Lorberboym, F. Wallach, L. Estok, R.E. Mosesson, M. Sacher, C.K. Kim, J. Machac, Thallium-201 retention in focal intracranial lesions for differential diagnosis of primary lymphoma and non-malignant lesions in AIDS patients, *J. Nucl. Med.* 39 (1997) 1366–1369.
- [41] L. Ramanna, A. Waxman, G. Binney, S. Waxman, J. Mirra, G. Rosen, Thallium-201 scintigraphy in bone sarcoma: comparison with gallium-67 and technetium-MDP in the evaluation of chemotherapeutic response, *J. Nucl. Med.* 31 (1990) 567–572.
- [42] P.M. Mauch, *Principles of Oncology*, Harper and Row, New York, 1983.
- [43] American Cancer Society Cancer Statistics 1991, *Cancer J. Clin.* 37 (1991).
- [44] I. Fogelman, *Bone Scanning in Clinical Practice*, Springer-Verlag, New York, 1987.
- [45] H.M. Chilton, R.L. Witcofski, *Pharmaceuticals in Medical Imaging*, Macmillan Publishing Co., New York, 1990.
- [46] S.S. Jurrison, J.J. Benedict, B.C. Elder, R. Whittle, E. Deutsch, *Inorg. Chem.* 22 (1983) 1332.
- [47] C.L. De Ligny, W.J. Gelsema, T.G. Tji, Y.M. Huigen, H.A. Vink, Bone seeking radiopharmaceuticals, *Nucl. Med. Biol.* 17 (1990) 161–179.
- [48] T.C. Pinkerton, W.R. Heinenian, E. Deutsch, Separation of technetium hydroxyethylidene diphosphonate complexes by anion exchange high-performance liquid chromatography, *Anal. Chem.* 52 (1980) 1106.
- [49] G.M. Wilson, T.C. Pinkerton, *Anal. Chem.* 57 (1985) 246.
- [50] Z.H. Oster, P. Som, S.C. Srivastava, R.G. Fairchild, G.E. Meinken, G.Y. Tillman, D.F. Sacker, P. Richards, H.L. Atkins, A.B. Brill, F.F. Knapp, T.A. Butler, The development and *in vivo* behavior of Sn containing radiopharmaceuticals. II. Autoradiographic and scintigraphic studies in normal animals and in animal models of bone disease, *Int. J. Nucl. Med. Biol.* 12 (1985) 175–184.
- [51] J. Ohiron, W.A. Volkert, J. Garlich, R.A. Holmes, Determination of lesion to normal bone uptake ratios of skeletal radiopharmaceuticals by QARG, *Nucl. Med. Biol.* 18 (1991) 235–240.
- [52] L. Rosenthal, J. Stern, A.A. Arzoumanian, A clinical comparison of MDP and DMAD, *Clin. Nucl. Med.* 7 (1982) 403–406.
- [53] M.L. Smith, W. Martin, J.H. McKillop, I. Fogelman, Improved lesion detection with dimethyl-amino-diphosphonate: A report of two cases, *Eur. J. Nucl. Med.* 9 (1984) 519–520.
- [54] P. Rigo, P. Paulus, B.J. Kaschten, R. Hustinx, T. Bury, G. Jerusalem, T. Benoit, J. Foidart-Willems, Oncological applications of positron emission tomography with fluorine-18 fluorodeoxyglucose, *Eur. J. Nucl. Med.* 23 (1996) 1641–1674.
- [55] T.A. Smith, FDG uptake, tumour characteristics and response to therapy: a review, *Nucl. Med. Commun.* 19 (1998) 97–105.
- [56] R.L. Wahi, R.L. Cody, G.D. Hutchins, E.E. Mudgett, Primary and metastatic breast carcinoma: initial clinical evaluation with PET and the radiolabeled glucose analog 2-[F-18]-fluoro-deoxy-2-D-glucose (FDG), *Radiology* 179 (1991) 3920–3925.
- [57] O.E. Nieweg, E.E. Kim, W.-H. Wong, W.F. Broussard, S.E.

- Singletary, G.N. Hortobagyi, R.S. Tilbury, Positron emission tomography with fluorine-18-deoxyglucose in the detection and staging of breast cancer, *Cancer* 71 (1993) 3920–3925.
- [58] P. Lindholm, H. Minn, S. Leskinen-Kallio, J. Bergman, U. Ruotsalainen, H. Joensuu, Influence of the blood glucose concentration on FDG uptake in cancer – a PET study, *J. Nucl. Med.* 34 (1993) 1–6.
- [59] R.A. Hawkins, M.E. Phelps, S.C. Huang, Effects of temporal sampling, glucose metabolic rats and disruptions of the blood-brain barrier on the FDG model with and without a vascular compartment: studies in human brain tumors with PET, *J. Cerebral Blood Flow Metab.* 6 (1986) 170–183.
- [60] G. Di Chiro, Positron emission tomography using [<sup>18</sup>F]fluorodeoxyglucose in brain tumors, a powerful diagnostic and prognostic tool, *Invest. Radiology* 22 (1987) 360–371.
- [61] K. Ishiwata, K. Kubota, M. Murakami, R. Kubota, M. Senda, A comparative study on protein incorporation of L-[methyl-<sup>3</sup>H]methionine, L-[1-<sup>14</sup>C]leucine and L-2-[<sup>18</sup>F]fluorotyrosine in tumor bearing mice, *Nucl. Med. Biol.* 20 (1993) 895–899.
- [62] M. Sasaki, Y. Ichiya, Y. Kuwabara, Ringlike uptake of [<sup>18</sup>F]FDG in brain abscess: a PET study, *J. Comp. Assis. Tomography* 14 (1990) 486–487.
- [63] R. Kubota, S. Yamada, K. Kubota, K. Ishiwata, N. Tamahashi, T. Ido, Intratumoral distribution of fluorine-18-fluorodeoxyglucose *in vivo*: high accumulation in macrophages and granulation tissues studied by microautoradiography, *J. Nucl. Med.* 33 (1992) 1972–1980.
- [64] R.L. Wahl, S.J. Fisher, A comparison of FDG, L-methionine and thymidine accumulation into experimental injections and reactive lymph nodes, *J. Nucl. Med.* 34 (1991) 104.
- [65] W. Vaalburg, H.H. Coenen, C. Crouzel, P.H. Elsinga, B. Langstrom, C. Lemaire, G.J. Meyer, Amino acids for the measurement of protein synthesis *in vivo* by PET, *Nucl. Med. Biol.* 19 (1992) 227–237.
- [66] K. Ishiwata, W. Vaalburg, P.H. Elsinga, A.M. Paans, M.G. Woldring, Comparison of L-[1-<sup>11</sup>C]methionine and L-methyl-[<sup>11</sup>C]methionine for measuring *in vivo* protein synthesis rats with PET, *J. Nucl. Med.* 29 (1988) 1419–1427.
- [67] K. Ishiwata, K. Kubota, M. Miurakami, R. Kubota, T. Sasaki, S. Ishii, M. Senda, Reevaluation of amino acid PET studies: can the protein synthesis rats in brain and tumor tissues be measured *in vivo*? *J. Nucl. Med.* 34 (1993) 1936–1943.
- [68] R. Huovinen, S. Leskinen-Kallio, K. Nagren, P. Lehkoinen, U. Ruotsalainen, M. Teras, Carbon-11-methionine and PET in evaluation of treatment response of breast cancer, *Br. J. Cancer* 67 (1993) 787–791.
- [69] K.-J. Langen, K. Ziemons, C.W. Jurgen, H.H. Kiwit, T. Kuwert, W.J. Bock, G. Stocklin, L.E. Feinendegen, H.-W.M. Gartner, 3-[<sup>123</sup>I]-Iodo- $\alpha$ -methyltyrosine and [methyl-<sup>11</sup>C]-L-methionine uptake in cerebral gliomas: a comparative study using SPECT and PET, *J. Nucl. Med.* 38 (1997) 517–522.
- [70] A.M.J. Paans, J. Pruijm, A. van Waarde, A.T.M. Willemsen, W. Vaalburg, Radiolabelled tyrosine for the measurement of protein synthesis rate *in vivo* by positron emission tomography, *Bailliere's Clin. Endocrin. Metab.* 10 (1996) 497–510.
- [71] J.A. Katzenellenbogen, R.E. Coleman, R.A. Hawkins, K.A. Krohn, S.M. Larson, J. Mendelsohn, C.K. Osborne, D. Pivnicka-Worms, R.C. Reba, B.A. Siegel, M.J. Welch, F. Shtern, Tumor receptor imaging: Proceedings of the National Cancer Institute Workshop, Review of Current Work, and Prospective for Further Investigations, *Clin. Cancer Res.* 1 (1995) 921–932.
- [72] C.L. Edwards, R.L. Hayes, Tumor scanning with <sup>67</sup>Ga citrate, *J. Nucl. Med.* 10 (1969) 103–105.
- [73] S.W. Gunesekeera, L.J. King, P.J. Lavender, The behavior of tracer gallium-67 towards serum proteins, *Clin. Chim. Acta* 39 (1972) 401–406.
- [74] R.E. Weiner, The mechanism of <sup>67</sup>Ga localization in malignant disease, *Nucl. Med. Biol.* 23 (1996) 745–751.
- [75] C.A. Luttrupp, J.A. Jackson, B.J. Jones, M.-H. Sohn, R.E. Lynch, K.A. Morton, Uptake of gallium-67 in transfected cells and tumors absent or enriched in the transferrin receptor, *J. Nucl. Med.* 39 (1998) 1405–1411.
- [76] M.A. Mintun, D.R. Dennis, M.J. Welch, C.J. Mathias, D.P. Schuster, Measurements of pulmonary vascular permeability with PET and gallium-68 transferrin, *J. Nucl. Med.* 28 (1987) 1704–1716.
- [77] D.M. Weiland, J. Wu, L.E. Brown, T.J. Mangner, D.P. Swanson, W.H. Beierwaltes, Radiolabeled adrenergic neuron-blocking agents: Adrenomedullary imaging with [<sup>131</sup>I]iodobenzylguanidine, *J. Nucl. Med.* 21 (1980) 349–353.
- [78] H. Sinzinger, F. Renner, S. Granegger, Unsuccessful iodine-131 MIBG imaging of carcinoid tumors and apudomas (letter), *J. Nucl. Med.* 27 (1986) 1221–1222.
- [79] J. Bomanji, J.L. Hungerford, J.E. Kingston, D.A. Levison, K.E. Brittin, <sup>123</sup>I metaiodobenzylguanidine (MIBG) scintigraphy of retinoblastoma: preliminary experience, *Br. J. Ophthalmol.* 73 (1989) 146–150.
- [80] A. Osei Bonsu, E.M. Kokoscbka, W. Ulrich, H. Sinzinger, <sup>131</sup>I-metaiodobenzylguanidine (MIBG) for bronchial oat cell cancer and melanoma detection, *Eur. J. Nucl. Med.* 15 (1989) 629–631.
- [81] N.A. Petry, B. Shapiro, *Pharmaceuticals in Medical Imaging*, Macmillan Publishing Co., New York, 1990.
- [82] J.V. Glowniak, J.E. Kilty, S.G. Amara, B.J. Hoffman, F.E. Turner, Evaluation of metaiodobenzylguanidine uptake by the norepinephrine, dopamine and serotonin transporters, *J. Nucl. Med.* 34 (1993) 1140–1146.
- [83] S. Jacques Jr., M.C. Tobes, J.C. Sisson, J.A. Baker, D.M. Wieland, Comparison of the sodium-dependency of uptake of meta-iodobenzylguanidine and norepinephrine into cultured bovine adrenomedullary cells, *Mol. Pharmacol.* 26 (1984) 539–546.
- [84] M.C. Tobes, S. Jacques Jr., D.M. Wieland, J.C. Sisson, Effect of uptake-one inhibitors on the uptake of norepinephrine and metaiodobenzylguanidine, *J. Nucl. Med.* 26 (1985) 897–907.
- [85] L. Von Moll, A.J. McEwan, B. Shapiro, J.C. Sisson, M.D. Gross, R. Lloyd, E. Beals, W.H. Beierwaltes, N.W. Thompson, Iodine-131-MIBG scintigraphy of neuroendocrine tumors other than pheochromocytoma and neuroblastoma, *J. Nucl. Med.* 28 (1987) 979–988.

- [86] B. Gasnier, M.P. Roisen, D. Scherman, S. Coornaert, G. Desplanones, J.P. Henry, Uptake of metaiodobenzylguanidine by bovine chromaffin granule membranes, *Mol. Pharmacol.* 29 (1985) 275–280.
- [87] S.D.J. Yeh, L. Helson, R.S. Benau, Correlation between iodine-131 MIBG imaging and biologic markers in advanced neuroblastoma, *Clin. Nucl. Med.* 13 (1988) 46–52.
- [88] B. De Bernardi, D. Rogers, M. Carli, E. Madon, T. de Laurentis, S. Bagnulo, M.T. di Tullio, G. Paolucci, G. Pastore, Localized neuroblastoma: surgical and pathologic staging, *Cancer* 60 (1987) 1066–1072.
- [89] R. Nitschke, E.I. Smith, S. Shochat, G. Altshuler, H. Travers, J.J. Shuster, Localized neuroblastoma treated by surgery: a pediatric oncology group study, *J. Clin. Oncol.* 6 (1988) 1271–1279.
- [90] G.M. Haase, K.Y. Wong, A.A. de Lorimier, H.N. Sather, G.D. Hammond, Improvement in survival after excision of primary tumor in stage III neuroblastoma, *J. Pediatr. Surg.* 24 (1989) 194–200.
- [91] K.K. Matthay, D. Stram, R.C. Seeger, J. Atkinson, H. Shimada, G.D. Hammond, A prospective childrens cancer group study of stage II neuroblastoma treated with surgery alone, *Proc. Am. Soc. Clin. Oncol.* 12 (1993) 414.
- [92] S. Tsuchimochi, M. Nakajo, Y. Nakabeppu, A. Tani, Metastatic pulmonary pheochromocytomas: positive I-123 MIBG SPECT with negative I-131 MIBG and equivocal I-123 MIBG planar imaging, *Clin. Nucl. Med.* 22 (1997) 687–690.
- [93] R. Guillemin, Peptides in the brain: the new endocrinology of the neuron, *Science* 202 (1978) 390–402.
- [94] S. Reichlin, Somatostatin (part 1), *New Engl. J. Med.* 309 (1983) 1495–1501.
- [95] S. Reichlin, Somatostatin (part 2), *New Engl. J. Med.* 309 (1983) 1556–1563.
- [96] J.C. Reubi, L.K. Kvols, E.P. Krenning, S.W.J. Lamberts, Distribution of somatostatin receptors in normal and tumor tissue, *Metabolism* 39(2) (1990) 78–81.
- [97] W. Bauer, U. Briner, W. Doepfner, R. Haller, R. Huguenin, P. Marbach, T.J. Petcher, J. Pless, SMS 201-995, *Life Sci.* 31 (1982) 1133–1140.
- [98] W.H. Bakker, R. Albert, C. Bruns, W.A.P. Breeman, L.J. Hofland, P. Marbach, J. Pless, D. Pralet, B. Stolz, J.W. Koper, S.W.J. Lamberts, T.J. Visser, E.P. Krenning, [<sup>111</sup>In-DTPA-D-Phe]-Octreotide, a potential radiopharmaceutical for imaging of somatostatin receptor-positive tumors: synthesis, radiolabeling and *in vitro* validation, *Life Sci.* 49 (1991) 1583–1591.
- [99] W.H. Bakker, E.P. Krenning, J.C. Reubi, W.A.P. Breeman, B. Setyono-Han, M. de Jong, J.C. Reubi, P.P.M. Kooij, C. Bruns, P.M. van Hagen, P. Marbach, T.J. Visser, J. Pless, S.W.J. Lamberts, *In vivo* application of [<sup>111</sup>In-111-DTPA-D-Phe]-Octreotide for detection of somatostatin receptor-positive tumors in rats, *Life Sci.* 49 (1991) 1593–1601.
- [100] E.P. Krenning, W.H. Bakker, P.P.M. Kooij, W.A.P. Breeman, H.Y. Oei, M. de Jong, J.C. Reubi, T.J. Visser, C. Bruns, D.J. Kwekkeboom, A.E.M. Reijs, P.M. van Hagen, J.W. Koper, S.W.J. Lamberts, Somatostatin receptor scintigraphy with indium-111-DTPA-D-Phe-1-Octreotide in man: metabolism, dosimetry and comparison with iodine-123-Tyr-3-Octreotide, *J. Nucl. Med.* 23 (1992) 652–658.
- [101] E.P. Krenning, D.J. Kwekkeboom, W.H. Bakker, W.A.P. Breeman, P.P.M. Kooij, H.Y. Oei, M. van Hagen, P.T.E. Postema, M. de Jong, J.C. Reubi, T.J. Visser, A.E.M. Reijs, L.J. Hofland, J.W. Koper, S.W.J. Lamberts, Somatostatin receptor scintigraphy with [<sup>111</sup>In-DTPA-D-Phe<sup>1</sup>]-and [<sup>123</sup>I-Tyr<sup>3</sup>]-octreotide: the rotterdam experience with more than 1000 patients, *Eur. J. Nucl. Med.* 20 (1993) 716–731.
- [102] C.J. Anderson, T.S. Pajean, W.B. Edwards, E.L.C. Sherman, B.E. Rogers, M.J. Welch, *In vitro* and *in vivo* evaluation of copper-64-labeled octreotide conjugates, *J. Nucl. Med.* 36 (1995) 2315–2325.
- [103] P.M. Smith-Jones, B. Stolz, C. Bruns, R. Albert, H.W. Reist, R. Fridrich, H.R. Mäcke, Gallium-67/gallium-68-[DFO]-octreotide – a potential radiopharmaceutical for PET imaging of somatostatin receptor-positive tumors: synthesis and radiolabeling *in vitro* and preliminary *in vivo* studies, *J. Nucl. Med.* 35 (1994) 317–325.
- [104] B. Stolz, P.M. Smith-Jones, R. Albert, H. Reist, H. Mäcke, C. Bruns, Biological characterization of [<sup>67</sup>Ga] or [<sup>68</sup>Ga] labelled DFO-octreotide (SDZ-216-927) for PET studies of somatostatin receptor positive tumors, *Horm. Metab. Res.* 26 (1994) 452–459.
- [105] H.-J. Wester, J. Brockmann, F. Rosch, W. Wutz, H. Herzog, P. Smith-Jones, B. Stolz, C. Bruns, G. Stocklin, PET-Pharmacokinetics of <sup>18</sup>F-octreotide: a comparison with <sup>67</sup>Ga-DFO- and <sup>86</sup>Y-DTPA-octreotide, *Nucl. Med. Biol.* 24 (1997) 275–286.
- [106] F. Dehdashti, C.J. Anderson, D.D. Trask, L.A. Bass, S.W. Schwarz, P.D. Cutler, D.W. McCarthy, M.V. Lanahan, Initial results with PET imaging using Cu-64-labeled TETA-Octreotide in patients with carcinoid tumor (abstract), *J. Nucl. Med.* 38 (1997) 103.
- [107] P.M. Smith-Jones, B. Stolz, R. Albert, G. Ruser, H. Mäcke, U. Briner, L. Tolsvai, G. Weckbecker, C. Bruns, Synthesis, radiolabelling, and evaluation of DTPA/octreotide conjugates for radiotherapy, *J. Label Comp. Radiopharm.* 37 (1995) 499–501.
- [108] M. de Jong, W.H. Bakker, E.P. Krenning, W.A.P. Breeman, M.E. van der Pluijm, B.F. Bernard, T.J. Visser, E. Jernann, M. Behe, P. Powell, H. Mäcke, Yttrium-90 and indium-111 labelling, receptor binding and biodistribution of [DOTA<sup>0</sup>,D-Phe<sup>1</sup>,Tyr<sup>3</sup>]octreotide, a promising somatostatin analogue for radionuclide therapy, *Eur. J. Nucl. Med.* 24 (1997) 368–371.
- [109] H. Herzog, F. Rösch, J. Brockmann, H. Muhlensiepen, M. Kohie, B. Stolz, P. Marbach, H.W. Muller-Gartner, Quantitative evaluation of Y-90-DOTA-Tyr<sup>3</sup>-octreotide as measured in baboons by means of yttrium-86 and PET, *J. Nucl. Med.* 38 (1997) 60.
- [110] B. Stolz, P. Smith-Jones, R. Albert, L. Tolcsvai, U. Briner, G. Ruser, H. Mäcke, G. Weckbecker, C. Bruns, Somatostatin analogues for somatostatin-receptor-mediated radiotherapy of cancer, *Digestion* 57(1) (1996) 17–21.
- [111] D.A. Pearson, J. Lister-James, W.J. McBride, D.M. Wilson, L.J. Martel, E.R. Civitello, J.E. Taylor, B.R. Moyer, R.T. Dean, Somatostatin receptor-binding peptides labeled with

- technetium-99m: chemistry and initial biological studies, *J. Med. Chem.* 39 (1996) 1361–1371.
- [112] S. Vallabhajosula, B.R. Moyer, J. Lister-James, B.J. McBride, H. Lipszyc, H. Lee, D. Bastidas, R.T. Dean, Preclinical evaluation of technetium-99m-labeled somatostatin receptor-binding peptides, *J. Nucl. Med.* 37 (1996) 1016–1022.
- [113] C.J. Palestro, R. Bitton, M.B. Tomas, D. Myssiorek, K.K. Bhargava, Y.M. Baran, P829: A technetium-labeled peptide for imaging tumors possessing somatostatin receptors, *J. Nucl. Med.* 38 (1997) 236.
- [114] M. de Jong, W.H. Bakker, W.A.P. Breeman, B.F. Bernard, L.J. Hofland, T.J. Visser, A. Srinivasan, M. Schmidt, M. Behe, H. Maecke, E.P. Krenning, Pre-clinical comparison of [DTPA<sup>0</sup>]Octreotide, [DTPA<sup>0</sup>Tyr<sup>3</sup>]Octreotide and [DOTA<sup>0</sup>Tyr<sup>3</sup>]Octreotide as carriers for somatostatin receptor-targeted scintigraphy and radionuclide therapy, *Int. J. Cancer* 75 (1998) 406–411.
- [115] M. de Jong, W.A.P. Breeman, W.H. Bakker, P.P.M. Kooij, B.F. Bernard, L.J. Hofland, T.J. Visser, A. Srinivasan, M. Schmidt, J.L. Erion, J.E. Bugaj, H.R. Maecke, E.P. Krenning, Comparison of <sup>111</sup>In-labeled somatostatin analogues for tumor scintigraphy and radionuclide therapy, *Cancer Res.* 58 (1998) 437–441.
- [116] J.S. Lewis, A. Srinivasan, M.A. Schmidt, C.J. Anderson, *In vitro* and *in vivo* evaluation of copper-64-TETA-Tyr<sup>3</sup>-Octreotate: somatostatin receptor binding studies, rodent biodistribution and primate PET imaging, *J. Nucl. Med.* 39 (1998) 63.
- [117] J.A. Katzenellenbogen, Designing steroid receptor-based radiotracers to image breast and prostate cancer, *J. Nucl. Med.* 36(S) (1995) 8–13.
- [118] J.A. Katzenellenbogen, K.D. McElvany, S.G. Senderoff, K.E. Carlson, S.W. Landvatter, M.J. Welch, [<sup>77</sup>Br]-16 $\alpha$ -bromoestradiol-17 $\beta$ : a high specific-activity gamma-emitting tracer with uptake in rat uterus and induced mammary tumors, *J. Nucl. Med.* 22 (1981) 42–47.
- [119] P.C. Pieslor, R.E. Gibson, W.C. Eckelman, K.K. Oates, B. Cook, R.C. Reba, Three radioligands compared for determining cytoplasmic estrogen-receptor content of human breast carcinomas, *Clin. Chem.* 28 (1982) 532–537.
- [120] K.D. McElvany, K.E. Carlson, M.J. Welch, *In vivo* Comparison of 16 $\alpha$ -[<sup>77</sup>Br]-bromoestradiol-17 $\beta$  and 16 $\alpha$ -[<sup>125</sup>I]-iodoestradiol-17 $\beta$ , *J. Nucl. Med.* 23 (1982) 420–424.
- [121] R.N. Hanson, L.A. Franke, Preparation and evaluation of 17 $\alpha$ -[<sup>125</sup>I]-iodovinyl-11 $\beta$ -methoxyestradiol as a highly selective radioligand for tissues containing estrogen receptors: concise communication, *J. Nucl. Med.* 25 (1984) 998–1002.
- [122] D.O. Kiesewetter, M.R. Kilbourn, S.W. Landvatter, D.F. Heiman, J.A. Katzenellenbogen, M.J. Welch, Preparation of four fluorine-18-labeled estrogens and their selective uptakes in target tissues of immature rats, *J. Nucl. Med.* 25 (1984) 1212–1221.
- [123] H.F. VanBrocklin, K.E. Carlson, J.A. Katzenellenbogen, M.J. Welch, 16 $\beta$ -[<sup>18</sup>F]fluoromoxestrol: a potent metabolically stable Positron Emission Tomography imaging agent for estrogen receptor positive human breast tumors, *Life Sci.* 53 (1993) 811–819.
- [124] A.H. McGuire, F. Dehdashti, B.A. Siegel, A.P. Lyss, J.W. Brodack, C.J. Mathias, M.A. Mintun, J.A. Katzenellenbogen, M.J. Welch, Positron tomographic assessment of 16 $\alpha$ s-[<sup>18</sup>F]Fluoro-17 $\beta$ -estradiol uptake in metastatic breast carcinoma, *J. Nucl. Med.* 32 (1991) 1526–1531.
- [125] C.M. Mendel, The free hormone hypothesis: a physiologically based mathematical model, *Endocrine Rev.* 10 (1989) 232–274.
- [126] D.J. Hyrb, M.S. Khan, N.A. Romas, W. Rosner, The control of the interaction of sex hormone-binding globulin with its receptor by steroid hormones, *J. Biol. Chem.* 265 (1990) 6048–6054.
- [127] S.D. Jonson, M.J. Welch, PET imaging of breast cancer with fluorine-18 radiolabeled estrogens and progestins, *Quart. J. Nucl. Med.* 42 (1998) 8–17.
- [128] A. Liu, J.A. Katzenellenbogen, H.F. VanBrocklin, C.J. Mathias, M.J. Welch, 20-[<sup>18</sup>F]fluoromibolone, a positron-emitting radiotracer for androgen receptors: synthesis and tissue distribution studies, *J. Nucl. Med.* 32 (1991) 81–88.
- [129] S. Liu, S.J. Rettig, C. Orvig, Polydentate ligand chemistry of group 13 metals: effects of the size and donor selectivity of metal ions on the structures and properties of aluminum, gallium and indium complexes with potentially heptadentate (N<sub>4</sub>O<sub>3</sub>) amine phenol ligands, *Inorg. Chem.* 31 (1992) 5400–5407.
- [130] T.A. Bonasera, J.P. O'Neil, M. Xu, J.A. Dobkin, P.D. Cutler, L.L. Lich, Y.S. Choe, J.A. Katzenellenbogen, M.J. Welch, Preclinical evaluation of fluorine-18-labeled androgen receptor ligands in baboons, *J. Nucl. Med.* 37 (1996) 1009–1015.
- [131] P.D. Cutler, F. Dehdashti, B.A. Siegel, J.B. Downer, M.J. Welch, Investigation of a prostate ligand 16 $\beta$ -[<sup>18</sup>F]Fluoro-5 $\alpha$ -dihydrotestosterone for staging of prostate carcinoma, *J. Nucl. Med.* 37 (1996) 87.
- [132] F. Dehdashti, J.E. Mortimer, B.A. Siegel, L.K. Griffeth, T.A. Bonasera, M.J. Fusselman, D.D. Detert, P.D. Cutler, J.A. Katzenellenbogen, M.J. Welch, Positron tomographic assessment of estrogen receptors in breast cancer: Comparison with FDG-PET and *in vitro* receptor assays, *J. Nucl. Med.* 36 (1995) 1766–1774.
- [133] J.E. Mortimer, F. Dehdashti, B.A. Siegel, J.A. Katzenellenbogen, P. Fracasso, M.J. Welch, Positron emission tomography with 2-[<sup>18</sup>F]Fluoro-2-deoxy-D-glucose and 16 $\alpha$ -[<sup>18</sup>F]-Fluoro-17 $\beta$ -estradiol in breast cancer: correlation with estrogen receptor status and response to systemic therapy, *Clin. Cancer Res.* 2 (1996) 933–939.
- [134] F.L. Flanagan, F. Dehdashti, J.E. Mortimer, B.A. Siegel, S.D. Jonson, M.J. Welch, PET assessment of response to tamoxifen therapy in patients with metastatic breast cancer, *J. Nucl. Med.* 37 (1996) 99.
- [135] J.A. Endicott, V. Ling, The biochemistry of P-glycoprotein mediated multidrug resistance, *Annu. Rev. Biochem.* 58 (1989) 137–171.
- [136] I.B.E. Roninson, *Molecular and Cellular Biology of Multi-drug Resistance in Tumor Cells*, Plenum Press, New York, 1991.

- [137] M.M. Gottesman, I. Pastan, Biochemistry of multidrug resistance mediated by the multidrug transporter, *Annu. Rev. Biochem.* 62 (1993) 385–427.
- [138] S.P.C. Cole, G. Bhardwaj, G.H. Gerlach, J.E. Mackie, C.E. Grant, K.C. Almquist, A.J. Stewart, E.U. Kurz, A.M.V. Duncan, R.G. Deelay, Overexpression of a transporter gene in a multidrug resistant human lung cancer cell line, *Science* 258 (1992) 1650–1654.
- [139] C.J. Chen, J.E. Chin, K. Ueda, D.P. Clark, I. Pastan, M.M. Gottesman, I.B. Roninson, Internal duplication and homology with bacterial transport proteins in the *mdr1* (P-glycoprotein) gene from multidrug-resistant human cells, *Cell* 47 (1986) 381–389.
- [140] P. Gros, J. Croop, I. Roninson, A. Varshavsky, D.E. Housman, Isolation and characterization of DNA sequences amplified in multidrug-resistant hamster cells, *Proc. Natl. Acad. Sci. U.S.A.* 83 (1986) 337–341.
- [141] T.P. Miller, T.M. Grogan, W.S. Dalton, C.M. Spier, R.J. Scheper, S.E. Salmon, P-glycoprotein expression in malignant lymphoma and reversal of clinical drug resistance with chemotherapy plus high-dose verapamil, *J. Clin. Oncol.* 9 (1991) 17–24.
- [142] J.M. Ford, W.N. Hait, Pharmacology of drugs that alter multidrug resistance in cancer, *Pharmacol. Rev.* 42 (1990) 155–199.
- [143] A.T. Fojo, K. Ueda, D.J. Slamon, D.G. Poplack, M.M. Gottesman, I. Pastan, Expression of a multidrug-resistance gene in human tumors and tissues, *Proc. Natl. Acad. Sci. U.S.A.* 84 (1987) 265–269.
- [144] D.D. Ross, B.W. Thompson, J.V. Ordonez, C.C. Joneckis, Improvement of flowcytometric detection of multidrug-resistant cells by cell-volume normalization of intracellular daunorubicin content, *Cytometry* 10 (1989) 185–191.
- [145] T.J. Lampidis, C. Castello, A. del Giglio, B.C. Pressman, P. Viallet, K.W. Trevorrow, G.K. Valet, H. Tapiero, N. Savaraj, Relevance of the chemical charge of rhodamine dyes to multiple drug resistance, *Biochem. Pharmacol.* 38 (1989) 4267–4271.
- [146] W.S. Dalton, T.M. Grogan, J.A. Rybski, R.J. Scheper, L. Richter, J. Kailley, H.J. Broxterman, H.M. Pinedo, S.E. Salmon, Immunohistochemical detection and quantification of P-glycoprotein in multiple drug-resistant human myeloma cells: association with level of drug resistance and drug accumulation, *Blood* 73 (1989) 747–752.
- [147] H. Chan, P. Thorner, G. Haddad, V. Ling, Immunohistochemical detection of P-glycoprotein: prognostic correlation in soft tissue sarcoma of childhood, *J. Clin. Oncol.* 8 (1990) 689–704.
- [148] P. Van der Valk, C.K. van Kalken, H. Ketelaars, H.J. Boxterman, G. Sheffer, C.M. Kuiper, T. Tsuruo, J. Lankelema, C.J. Meijer, H. Pinedo, R. Scheper, Distribution of multi-drug resistance-associated P-glycoprotein in normal and neoplastic human tissues, *Annal. Oncol.* 1 (1990) 56–64.
- [149] D. Kessel, W.T. Beck, T. Kukuruga, V. Schulz, Characterization of multidrug resistance by fluorescent dyes, *Cancer Res.* 51 (1991) 4665–4670.
- [150] K.E. Noonan, C. Beck, T.A. Holzmayer, J.E. Chin, J.S. Wunder, I.L. Andrulis, A.F. Gazdar, C.L. Willman, B. Griffith, D. Von Hoff, Quantitative analysis of MDRa (multidrug resistance) gene expression in human tumors by polymerase chain reaction, *Proc. Natl. Acad. Sci. U.S.A.* 87 (1990) 7160–7164.
- [151] A.G. Jones, M.J. Abrams, A. Davison, J.W. Brodack, A.K. Toothaker, S.J. Adestein, A.I. Kassiss, Biological studies of a new class of technetium complexes: the hexakis(alkylisonitrile)technetium(I) cations, *Int. J. Nucl. Med. Biol.* 11 (1984) 225–234.
- [152] D. Piwnica-Worms, M.L. Claiu, M. Budding, J.F. Kronauge, R.A. Kramer, J.M. Croop, Functional imaging of multidrug-resistant P-glycoprotein with an organotechnetium complex, *Cancer Res.* 53 (1993) 977–984.
- [153] D. Piwnica-Worms, V.V. Rao, J.F. Kronauge, J.M. Croop, Characterization of multidrug resistance P-glycoprotein transport function with an organotechnetium cation, *Biochemistry* 34 (1995) 12210–12220.
- [154] J.R. Ballinger, K.M. Sheldon, I. Boxen, C. Erlichman, V. Ling, Differences between accumulation of  $^{99m}\text{Tc}$ -MIBI and  $^{201}\text{Tl}$ -thallous chloride in tumour cells: role of P-glycoprotein, *Quart. J. Nucl. Med.* 39 (1995) 122–1228.
- [155] M.D. Cordobes, A. Starzec, L. Delmon-Moingeon, C. Blanchot, J.C. Kouyoumdjian, G. Prevost, M. Caglar, J.L. Moretti, Technetium-99m-sestamibi uptake by human benign and malignant breast tumor cells: Correlation with *mdr* gene expression, *J. Nucl. Med.* 37 (1996) 286–289.
- [156] I. Bosch, C.L. Crankshaw, D. Piwnica-Worms, J.M. Croop, Characterization of functional assays of multidrug resistance P-glycoprotein transport activity, *Leukemia* 11 (1997) 1131–1137.
- [157] S. Del-Vecchio, A. Ciarniello, M.I. Potena, M.V. Carriero, C. Mainolfi, G. Botti, R. Thomas, M. Cerra, G. D'Aiuto, T. Tsuruo, M. Salvatore, *In vivo* detection of multidrug-resistant (MDR1) phenotype by technetium-99m sestamibi scan in untreated breast cancer patients, *Eur. J. Nucl. Med.* 24 (1997) 150–159.
- [158] G.D. Luker, P.M. Fracasso, J. Dobkin, D. Piwnica-Worms, Modulation of the multidrug resistance P-glycoprotein: Detection with technetium-99m-sestamibi *in vivo*, *J. Nucl. Med.* 38 (1997) 369–372.
- [159] J.E. Moulder, S. Rockwell, Tumor hypoxia: its impact on cancer therapy, *Br. J. Radiol.* 26 (1987) 638–648.
- [160] S. Rockwell, S.R. Keyes, A.C. Sartorelli, Preclinical studies of porfiromycin as an adjunct to radiotherapy, *Radiat. Res.* 116 (1988) 100–113.
- [161] S. Rockwell, Effect of some proliferative and environmental factors on the toxicity of mitomycin C to tumor cells *in vitro*, *Int. J. Cancer* 38 (1986) 229–235.
- [162] C.N. Coleman, Hypoxia in tumors: A paradigm for the approach to biochemical and physiological heterogeneity, *J. Natl. Cancer Inst.* 80 (1988) 310–317.
- [163] L.J. Peters, H.R. Withers, H.D. Thames, G.H. Fletcher, Keynote address – the problem: Tumor radioresistance in clinical radiotherapy, *Int. J. Radiat. Oncol. Biol. Phys.* 8 (1982) 101–108.
- [164] W.L. Rumsey, B. Patel, K. Linder, Effect of graded hypoxia in retention of technetium-99m-nitroheterocycle in perfused rat hearts, *J. Nucl. Med.* 36 (1995) 632–636.
- [165] G.J.R. Cook, S. Houston, S.F. Barrington, I. Fogelman,

- Technetium-99m-labeled HL91-to identify tumor hypoxia: Correlation with fluorine-18-FDG, *J. Nucl. Med.* 39 (1998) 99–103.
- [166] C.J. Mathias, M.J. Welch, M.R. Kilbourn, P.A. Jerabek, T.B. Patrick, M.E. Raichle, K.A. Krohn, J.S. Rasey, D.W. Shaw, Radiolabeled hypoxic cell sensitizers: Tracers for assessment of ischemia, *Life Sci.* 41 (1987) 199–206.
- [167] J.M. Hoffman, J.S. Rasey, A.M. Spence, D.W. Shaw, K.A. Krohn, Binding of the hypoxic tracer [<sup>3</sup>H] misonidazole in cerebral ischemia, *Stroke* 18 (1987) 168–176.
- [168] G.V. Martin, J.H. Caldwell, M.M. Graham, J.R. Grierson, K. Kroll, M.J. Cowan, T.K. Lewellen, J.S. Rasey, J.J. Casciari, K.A. Krohn, Non-invasive detection of hypoxic myocardium using fluorine-18-fluoromisonidazole and Positron Emission Tomography, *J. Nucl. Med.* 33 (1992) 2202–2208.
- [169] M.E. Shelton, C. Dence, D.-R. Hwang, M.J. Welch, Myocardial kinetics of fluorine-18 misonidazole: a marker of hypoxic myocardium, *J. Nucl. Med.* 30 (1989) 351–358.
- [170] W.J. Koh, K.S. Bergman, J.S. Rasey et al, Evaluation of oxygenation status during fractionated radiotherapy in human non-small cell lung cancers using [F-18]fluoromisonidazole and Positron Emission Tomography, *Int. J. Radiat. Oncol. Biol. Phys.* 33 (1995) 391–398.
- [171] A. Nunn, K. Linder, H.W. Strauss, Nitroimidazoles and imaging hypoxia, *Eur. J. Nucl. Med.* 22 (1995) 265–280.
- [172] K.E. Linder, Y.W. Chan, J.E. Cyr, D.P. Nowotnik, W.C. Eckelman, A.D. Nunn, Synthesis, characterization, and *in vitro* evaluation of nitroimidazole-BATO complexes: new technetium compounds designed for imaging hypoxic tissue, *Bioconjugate Chem.* 4 (1993) 326–333.
- [173] C.K. Ng, A.J. Sinusas, B.L. Zaret, R. Soufer, Kinetic analysis of technetium-99m-labeled nitroimidazole (BMS-181321) as a tracer of myocardial hypoxia, *Circulation* 92 (1995) 1261–1268.
- [174] W.L. Rumsey, J.E. Cyr, N. Raju, R.K. Narra, A novel [99m]technetium-labeled nitroheterocycle capable of identification of hypoxia in heart, *Biochem. Biophys. Res. Commun.* 193 (1993) 1239–1246.
- [175] C.K. Stone, T. Mulix, R.J. Nickles, B. Renstrom, S.H. Nellis, A.J. Leidtke, A.D. Nunn, B.L. Kuczynski, W.L. Ramsey, Myocardial kinetics of a putative hypoxic tissue marker <sup>99m</sup>Tc-labeled nitroimidazole (BMS-181321), after regional ischemia and reperfusion, *Circulation* 92 (1995) 1246–1253.
- [176] W.L. Rumsey, B. Patel, K.E. Linder, Effect of graded hypoxia on retention of technetium-99m-nitroheterocycle in perfused rat heart, *J. Nucl. Med.* 36 (1995) 632–636.
- [177] R.D. Okada, K.N. Nguyen, M. Lauinger, I.L. Allton, G.R. Johnson, Technetium-99m-Q12 kinetics in perfused rat myocardium: effects of hypoxia and low flow, *Am. Heart. J.* 132 (1996) 108–115.
- [178] J.R. Ballinger, J.W. Kee, A.M. Rauth, *In vitro* and *in vivo* evaluation of a technetium-99m-labeled 2-nitroimidazole (BMS-181321) as a marker of tumor hypoxia, *J. Nucl. Med.* 37 (1996) 1023–1031.
- [179] K.E. Linder, Y.W. Chan, J.E. Cyr, M.F. Malley, D.P. Nowotnik, A.D. Nunn, TcO(PnAO-1-(2-nitroimidazole)) [BMS-181321], a new technetium-containing nitroimidazole complex for imaging hypoxia: synthesis, characterization, and xanthine oxidase-catalyzed reduction, *J. Med. Chem.* 37 (1994) 9–17.
- [180] P. Wedeking, F. Yost, M. Vven, B. Patel, S. Eaton, V. Romero, K.E. Lindner, W. Rumsey, A.D. Nunn, Comparison of the biological activity of the isomers of the Tc-99m-Nitroimidazole complex BMS-194796, *J. Nucl. Med.* 36 (1995) 17.
- [181] C.M. Archer, B. Edwards, J.D. Kelly, A.C. King, J.F. Burke, A.L.M. Riley, Technetium labelled agents for imaging hypoxia *in vivo*, in: M. Nicolini, G. Bandoli, U. Mazzi (Eds.), *Technetium and Rhenium in Chemistry and Nuclear Medicine* 4, SG Editoriali, Padova, Italy, 1995.
- [182] R.D. Okada, G. Johnson, K.N. Nguyen, B. Edwards, C.M. Archer, J.D. Kelly, *Circulation* 8S (1997) 1892–1899.
- [183] G.J.R. Cook, S. Houston, S.F. Barrington, I. Fogelman, Technetium-99m-labeled HL91 to identify tumor hypoxia: correlation with fluorine-18-FDG, *J. Nucl. Med.* 39 (1998) 99–103.
- [184] Y. Fujibayashi, K. Matsumoto, Y. Yonekura, J. Konishi, A. Yokoyama, A new zinc-62/copper-62 generator as a copper-62 source for PET radiopharmaceuticals, *J. Nucl. Med.* 30 (1989) 1838–1842.
- [185] Y. Fujibayashi, H. Taniuchi, N. Tajima, Y. Yonekura, J. Konishi, A. Yokoyama, New non-nitroimidazole hypoxia imaging agents, Cu-62-dithiosemicarbazone complexes with low redox potential, *J. Nucl. Med.* 36 (1995) 49.
- [186] J.L.J. Dearling, J.S. Lewis, G.E.D. Mullen, M.T. Rae, J. Zweit, P.J. Blower, Design of hypoxia-targeting radiopharmaceuticals: selective uptake of copper-64 complexes in hypoxic cells *in vitro*, *Eur. J. Nucl. Med.* 25 (1998) 788–792.
- [187] Y. Fujibayashi, C.S. Cutler, C.J. Anderson, D.W. McCarthy, L.A. Jones, T. Sharp, Y. Yonekura, M.J. Welch, Comparative imaging studies of <sup>64</sup>Cu-ATSM a hypoxia imaging agent and C-11-acetate in an acute myocardial infarction model: *ex vivo* imaging in rats, *Nucl. Med. Biol.* (in press).
- [188] J.S. Lewis, D.W. McCarthy, T.J. McCarthy, Y. Fujibayashi, M.J. Welch, The evaluation of <sup>64</sup>Cu-diacetyl-bis(*N*<sup>4</sup>-methylthiosemicarbazone)(<sup>64</sup>Cu-ATSM): *in vitro* and *in vivo* in a hypoxic tumor model, *J. Nucl. Med.* (in press).
- [189] Y. Fujibayashi, H. Taniuchi, Y. Yonekura, H. Ohtani, J. Konishi, A. Yokoyama, Copper-62-ATSM: A new hypoxia imaging agent with high membrane permeability and low redox potential, *J. Nucl. Med.* 38 (1997) 1115–1160.
- [190] H. Taniuchi, Y. Fujibayashi, H. Okazawa, Y. Yonekura, J. Konishi, A. Yokoyama, Cu-pyruvaldehyde-bis(*N*<sup>4</sup>-methylthiosemicarbazone) (Cu-PTSM), a metal complex with selective NADH-dependent reduction by complex 1 in brain mitochondria: A potential radiopharmaceutical for mitochondria-functional imaging with positron emission tomography, *Biol. Pharm. Bull.* 18 (1995) 1126–1129.
- [191] C.M. Lederer, V.S. Shirley (Eds.), *Table of Isotopes*, John Wiley and Sons, Inc., 1978.
- [192] C. Loc'h, B. Mazière, D. Comar, A new generator for ionic gallium-68, *J. Nucl. Med.* 21 (1979) 171–173.